ISSN 1949-8470 (online)

World Journal of *Radiology*

World J Radiol 2023 September 28; 15(9): 256-280

Published by Baishideng Publishing Group Inc

World Journal of Radiology

Contents

Monthly Volume 15 Number 9 September 28, 2023

REVIEW

CASE REPORT

World Journal of Radiology

Monthly Volume 15 Number 9 September 28, 2023

Contents

ABOUT COVER

Editorial Board Member of *World Journal of Radiology*, Alberto Tagliafico, MD, Assistant Professor, Department of Health Sciences (DISSAL), University of Genova, Genova 16138, Italy. alberto.tagliafico@unige.it

AIMS AND SCOPE

The primary aim of *World Journal of Radiology* (*WJR*, *World J Radiol*) is to provide scholars and readers from various fields of radiology with a platform to publish high-quality basic and clinical research articles and communicate their research findings online.

WJR mainly publishes articles reporting research results and findings obtained in the field of radiology and covering a wide range of topics including state of the art information on cardiopulmonary imaging, gastrointestinal imaging, genitourinary imaging, musculoskeletal imaging, neuroradiology/head and neck imaging, nuclear medicine and molecular imaging, pediatric imaging, vascular and interventional radiology, and women's imaging.

INDEXING/ABSTRACTING

The *WJR* is now abstracted and indexed in PubMed, PubMed Central, Emerging Sources Citation Index (Web of Science), Reference Citation Analysis, China National Knowledge Infrastructure, China Science and Technology Journal Database, and Superstar Journals Database. The 2023 Edition of Journal Citation Reports® cites the 2022 impact factor (IF) for *WJR* as 2.5; IF without journal self cites: 2.3; 5-year IF: 2.5; Journal Citation Indicator: 0.54.

RESPONSIBLE EDITORS FOR THIS ISSUE

Production Editor: *Si Zhao*; **Production Department Director:** *Xu Guo*; **Editorial Office Director:** *Jia-Ping Yan*.

NAME OF JOURNAL
World Journal of Radiology

ISSN
ISSN 1949-8470 (online)

LAUNCH DATE
January 31, 2009

FREQUENCY
Monthly

EDITORS-IN-CHIEF
Thomas J Vogl

EDITORIAL BOARD MEMBERS
https://www.wjgnet.com/1949-8470/editorialboard.htm

PUBLICATION DATE
September 28, 2023

INSTRUCTIONS TO AUTHORS
https://www.wjgnet.com/bpg/gerinfo/204

GUIDELINES FOR ETHICS DOCUMENTS
https://www.wjgnet.com/bpg/GerInfo/287

GUIDELINES FOR NON-NATIVE SPEAKERS OF ENGLISH
https://www.wjgnet.com/bpg/gerinfo/240

PUBLICATION ETHICS
https://www.wjgnet.com/bpg/GerInfo/288

PUBLICATION MISCONDUCT
https://www.wjgnet.com/bpg/gerinfo/208

ARTICLE PROCESSING CHARGE
https://www.wjgnet.com/bpg/gerinfo/242

STEPS FOR SUBMITTING MANUSCRIPTS
https://www.wjgnet.com/bpg/GerInfo/239

ONLINE SUBMISSION
https://www.f6publishing.com

World Journal of Radiology

Submit a Manuscript: https://www.f6publishing.com

World J Radiol 2023 September 28; 15(9): 256-273

DOI: 10.4329/wjr.v15.i9.256

ISSN 1949-8470 (online)

REVIEW

Role of pulmonary perfusion magnetic resonance imaging for the diagnosis of pulmonary hypertension: A review

Miriam Lacharie, Adriana Villa, Xenios Milidonis, Hadeer Hasaneen, Amedeo Chiribiri, Giulia Benedetti

Specialty type: Radiology, nuclear medicine and medical imaging

Provenance and peer review: Unsolicited article; Externally peer reviewed.

Peer-review model: Single blind

Peer-review report's scientific quality classification

Grade A (Excellent): 0
Grade B (Very good): 0
Grade C (Good): C, C
Grade D (Fair): 0
Grade E (Poor): 0

P-Reviewer: Liu YJ, Taiwan; Xu L, China

Received: July 27, 2023
Peer-review started: July 27, 2023
First decision: September 4, 2023
Revised: September 16, 2023
Accepted: September 22, 2023
Article in press: September 22, 2023
Published online: September 28, 2023

Miriam Lacharie, Oxford Centre of Magnetic Resonance Imaging, University of Oxford, Oxford OX3 9DU, United Kingdom

Adriana Villa, Department of Diagnostic and Interventional Radiology, German Oncology Centre, Limassol 4108, Cyprus

Xenios Milidonis, Deep Camera MRG, CYENS Centre of Excellence, Nicosia, Cyprus, Nicosia 1016, Cyprus

Hadeer Hasaneen, School of Biomedical Engineering & Imaging Sciences, King's College London, London WC2R 2LS, United Kingdom

Amedeo Chiribiri, School of Biomedical Engineering and Imaging Sciences, Kings Coll London, Div Imaging Sci, St Thomas Hospital, London WC2R 2LS, United Kingdom

Giulia Benedetti, Department of Cardiovascular Imaging and Biomedical Engineering, King's College London, London WC2R 2LS, United Kingdom

Corresponding author: Miriam Lacharie, MSc, Researcher, Oxford Centre of Magnetic Resonance Imaging, University of Oxford, John Radcliffe Hospital, Headington, Oxford OX3 9DU, Oxford OX3 9DU, United Kingdom. miriam.lacharie@cardiov.ox.ac.uk

Abstract

Among five types of pulmonary hypertension, chronic thromboembolic pulmonary hypertension (CTEPH) is the only curable form, but prompt and accurate diagnosis can be challenging. Computed tomography and nuclear medicine-based techniques are standard imaging modalities to non-invasively diagnose CTEPH, however these are limited by radiation exposure, subjective qualitative bias, and lack of cardiac functional assessment. This review aims to assess the methodology, diagnostic accuracy of pulmonary perfusion imaging in the current literature and discuss its advantages, limitations and future research scope.

Key Words: Pulmonary perfusion MRI; Pulmonary hypertension; Dynamic contrast enhanced magnetic resonance imaging; Chronic thromboembolic pulmonary hypertension; Computed tomography pulmonary angiography; Chronic thromboembolic disease

Core Tip: Chronic thromboembolic pulmonary hypertension is an under-diagnosed disorder with high mortality if not diagnosed on time, however it can be fully cured with efficient diagnostic tools. Pulmonary perfusion magnetic resonance imaging (MRI) provides a non-invasive, reliable, radiation free and safer diagnostic test potentially replacing the standard techniques. Cardiopulmonary MRI also provides a comprehensive cardiopulmonary assessment in one single visit resulting in patients' convenience and better utilization of healthcare resources and time.

Citation: Lacharie M, Villa A, Milidonis X, Hasaneen H, Chiribiri A, Benedetti G. Role of pulmonary perfusion magnetic resonance imaging for the diagnosis of pulmonary hypertension: A review. *World J Radiol* 2023; 15(9): 256-273
URL: https://www.wjgnet.com/1949-8470/full/v15/i9/256.htm
DOI: https://dx.doi.org/10.4329/wjr.v15.i9.256

INTRODUCTION

Pulmonary perfusion is crucial for the assessment of lung function, since proper pulmonary blood flow (PBF) and pulmonary ventilation are prerequisites for effective gas exchange. Pulmonary perfusion can be assessed by measuring mean pulmonary artery pressure (mPAP), pulmonary venous resistance (PVR), and pulmonary artery wedge pressure (PAWP) during right heart catheterization (RHC).

This normal pulmonary perfusion and ventilation pattern can be altered by several physiological and pathological conditions, including vascular (as in cases of chronic pulmonary thromboembolic disease - CTED) and parenchymal alterations (as in cases of lung fibrosis)[1]. These situations can lead to pulmonary hypertension (PH), PH is defined as mPAP of > 20 mmHg and PVR > 2.0 Woods Units[2].

PH is not a single entity, but rather a spectrum of disorders and can be due to multifactorial underlying pathophysiological mechanisms. Current guidelines classify PH in five types based on clinical presentation and aetiology: pulmonary arterial hypertension (PAH), PH due to left heart disease, PH due to lung disease, PH due to CTED (CTEPH) and PH due to unknown mechanisms (*e.g.*, associations include sarcoidosis, sickle cell anaemia, metabolic disorders, and others). Among all PH subtypes, CTEPH is the only treatable form; therefore, early, and accurate differential diagnosis is critical for therapy and prognosis[3,4].

CTEPH is caused by the chronic occlusion of pulmonary arteries due to thromboembolic material with subsequent increased mPAP and PVR, potentially leading to right heart failure and death if left untreated[5,6]. Risk factors for pulmonary thromboembolic vessel occlusion are age over 70, female gender, pulmonary embolism at first venous thromboembolic event, deep vein thrombosis, chronic obstructive pulmonary disease, heart failure and atrial fibrillation [7]. This article will discuss contemporary diagnostic methods to diagnose PH, what methods have been researched so far in medical literature and their diagnostic accuracy. It further explores advantages and limitations of current methods routinely used in clinical practice. It also discusses newly emerging techniques and future horizons of research in PH diagnosis.

Current imaging modalities used for PH diagnosis

Currently, the differential diagnosis of PH involves a multimodality approach including RHC, echocardiography, nuclear medicine based planer ventilation/perfusion scintigraphy scan (V/Q), single photon emission computed tomography (SPECT) scintigraphy and more recently a hybrid approach of combining SPECT and conventional computed tomography (SPECT-CT) scan[8]. All nuclear medicine techniques involve intravenous injection of radionuclide which emits gamma rays after reaching the region of interest in the body. These gamma rays are detected by gamma cameras providing functional assessment of lungs.

Planer scintigraphy has been largely replaced by SPECT because in SPECT gamma cameras rotate over a 360-degree arc around the patient providing three dimensional images which are crucial to detect small segmental perfusion defects.

Recently, hybrid SPECT-CT has also been used for clinical practice. It involves two different types of scans at the same time, a nuclear medicine scan involving radionuclide aerosol of technetium-99m diethylenetriaminepentaacetic acid delivered through a non-breathing mask which reaches to the distal tracheobronchial tree to reflect regional ventilation. Second part of study is an intravenous injection of TC-99m macro aggregates which gets lodged in pulmonary precapillary arterioles to provide pulmonary perfusion assessment *via* gamma camera[9,10]. At the same time, conventional CT scanner built in with the SPECT scintigraphy machine provides the anatomical details. Consequently, hybrid SPECT-CT can be considered superior to planar scintigraphy and SPECT alone.

Additionally, computed tomography pulmonary angiography (CTPA) has also been demonstrated to accurately detect pulmonary embolism, however it lacks the ability of dynamic pulmonary perfusion to detect perfusion defects at segmental and sub segmental pulmonary level. CTPA involves intravenous injection of iodine-based contrast injection and imaging of pulmonary arteries for the detection of contrast filling defect denoting pulmonary embolism.

Sensitivity and specificity of CTPA for pulmonary embolism varies from 83% to 100% and with recent advancements in SPECT the potential for routinely used modalities for CTEPH detection has been validated for pulmonary perfusion defect detection[11,12]. This is made possible by the high image resolution offered by multi slice CT scanning, allowing an accurate assessment of the location and severity of thromboembolic material up to the sub-segmental level, providing crucial information for the assessment of patients with CTEPH considered suitable for pulmonary endarterectomy (PEA)

[13]. Recently, dual energy computed tomography (CT) has further improved the assessment of patients with PH, thanks to the assessment of regional pulmonary perfusion with iodine perfusion maps[14].

Visual assessment of SPECT scintigraphy, SPECT-CT scintigraphy and CTPA images by expert radiologists is the routine clinical practice to identify partially or completely occluded pulmonary vessels and to assess lung perfusion.

Limitations of CTPA, V/Q scan and SPECT scintigraphy

Routine clinical tests for PH diagnosis are limited by radiation exposure causing carcinogenic stochastic effects (long-term cancer-causing effects after radiation exposure) and rarely deterministic effects (acute high dose exposure if radiation dose exceeds 100 mGy leading to skin erythema, organ damage/failure)[15]. However, these effects are extremely rare due to sophisticated equipment and specialised radiation dose lowering parameters.

The concern is exacerbated for women of child-bearing age, particularly considering the high female-to-male ratio (4.8:1) of incidence and prevalence of PH worldwide and harmful effects on foetal organogenesis[16,17]. Moreover, periodical follow-up to assess the disease progression is vital for PH management, imposing further radiation exposure.

The average effective radiation dose of V/Q scan has been estimated as 1.29 mSv, breast absorbed dose 0.37 mGy, uterus-absorbed dose 0.46 mGy and foetal absorbed doses of 0.40 mGy[18]. SPECT scintigraphy uses radionuclide doses of 25 to 30 MBq for ventilation and 100-120 MBq is usually required for a successful perfusion study[9,19].

Another limitation of current techniques like CTPA is ionising radiation exposure. The effective radiation dose of CTPA has been estimated to be 21 mSv and breast absorbed dose from 44 mGy to as high as 70 mGy to radiosensitive breast tissue[18,20]. Potential carcinogenic ionising radiation exposure and the need for frequent follow-up assessments by conventional tests for PH patients are a few limitations of current imaging tests for pulmonary embolism-based PH diagnosis[21].

Furthermore, as PH can inevitably affect cardiac functions, a single test including the assessment of left and right ventricular function and myocardial tissue characterisation would be desirable for a comprehensive assessment.

In a relevant study, researchers validated that cardiac magnetic resonance imaging (MRI) derived pulmonary artery pressure ejection fraction, RV stroke volume, cardiac output, ventricular mass index and pulmonary blood flow in non-treated lobes correlated with pulmonary blood flow changes in treated lobes post balloon pulmonary angioplasty $P < 0.05$. Furthermore, utility of pulmonary artery pulsatility and pulmonary artery flow measurement by cardiac MRI as an early marker of pulmonary hypertension has also been verified in another prospective study[22]. Therefore, these studies emphasize the significance of a comprehensive, non-invasive and ionising radiation free cardiopulmonary assessment using cardiac magnetic resonance and pulmonary MRI in a single setting.

Finally, in clinical practice these imaging tests are assessed visually only, which is prone to an observer-dependent evaluation, and the availability of quantitative analysis techniques could provide additional value.

Need of improved imaging assessment of CTEPH

Unfortunately, CTEPH retains high mortality, and the mean life expectancy has been reported as less than three years if left untreated[3,23]. Currently, CTEPH can be treated with PEA, which consists of the surgical resection of the thromboembolic material. Before PEA, the three-year mortality of CTEPH was over 50%[24]. It has been demonstrated that PEA can lead to significant improvements in hemodynamic and exercise capacity[23]. Delayed treatment however is still associated with poor prognosis, therefore early detection of CTEPH is critical[25].

A prospective European study of 679 patients with CTEPH, of which 386 underwent PEA, reported an in-hospital mortality rate as low as 4.7% and 1-year mortality of 7%, while the exercise capacity and pulmonary vascular resistance were significantly improved[26]. In another study, the mortality rate in 1500 consecutive CTEPH patients post PEA was investigated between 1999 and 2010. Outcomes were compared between historical cohorts and more recent patients, who received surgical treatment for distal disease affecting smaller pulmonary vessels. A significant reduction of mortality rate from 5.2% to 2.2% was observed, despite the more distal disease, reflecting a continuous improvement in surgical techniques and highlighting the need for more sensitive tests capable of identifying distal disease[27].

Most of CTEPH patients in these studies stated remarkable relief from symptoms after PEA and a return to near normal hemodynamic values[26-28]. These promising results of surgical treatment support the quest for new diagnostic methods capable of early differential diagnosis and further developments of surgical techniques for targeted intervention. Moreover, improved diagnostic tools are necessary for differentiating CTEPH from the other four types of PH because treatment pathways vary accordingly. Currently, this differentiation is based only on imaging tests that employ ionising radiations.

Recently, pulmonary perfusion MRI has been emerged as a powerful tool for the assessment of pulmonary hypertension, and particularly for the differential diagnosis of CTEPH[29]. Perfusion MRI can be performed using dynamic contrast imaging or without contrast using arterial spin labelling[30].

The aim of this review article is to provide an overview of the published studies on lung perfusion MRI, highlighting the limitations of standard tests and the role of perfusion MRI as a diagnostic tool for PH. Moreover, the review focuses on the methodology, advantages, challenges, and future directions for pulmonary perfusion MRI and its potential contribution to overall healthcare policies.

LITERATURE SEARCH

A comprehensive literature search was performed using, PubMed, EMBASE and Medline databases. To develop the literature search question, a PICO framework was adopted: Population; PH patients, Intervention; MRI, Comparison;

SPECT/CTPA, Outcome; diagnostic accuracy. Original prospective and retrospective studies were included in the literature search with or without direct comparison of pulmonary perfusion MRI to gold standard tests for the diagnosis of PH[31-55] in Table 1. Tables 2-4 provide the PICO framework, eligibility criteria for included studies and facet analysis with search strategy respectively. Figure 1 demonstrates the PRSMA flow chart for literature search.

Note that the acronym "Dynamic contract enhanced MRI (DCE-MRI)" was frequently used in the selected studies instead of pulmonary perfusion MRI.

Pulmonary perfusion MRI - methodology

MRI uses the interaction between a magnetic field, hydrogen ions in the body and radiofrequency pulses to generate diagnostic images in multiple planes with high spatial resolution and without the need for ionising radiation. An MRI sequence involves repeated application of radiofrequency pulses to the magnetized hydrogen ions in the body and measuring the MRI signals while the hydrogen ions are demagnetized over time (echo time, TE)[56]. Because of the inherent difference in magnetic susceptibility between lung parenchyma and air, MRI of lungs is prone to wider frequency distribution and phase dispersion, leading to suboptimal noisy images[57]. To mitigate this susceptibility effect, recent advancements in lung MRI are ultra-short echo and zero echo time acquisitions, allowing accelerated scan time whilst preserving optimal image quality[58,59].

For fast pulmonary vasculature imaging, gradient pulse sequences with short radiofrequency repetition time and short time to receive the signal are typically employed, which allows acquisition of dynamic images of the lungs in real time as contrast agent flows through the pulmonary vasculature[60] (Figure 2[34]).

A commonly used gradient echo pulse sequence for perfusion MRI is 3-dimensional fast low angle shot (FLASH) MRI acquiring dynamic perfusion images of lungs[61]. The dynamic visualisation of the first pass of the contrast agent across the pulmonary circulation is a crucial requirement for the assessment of lung perfusion[61,62].

Several studies have used 3D FLASH perfusion MRI for the detection of chronic thromboembolic disease[33,34,37,63]. However, 3D FLASH perfusion MRI is limited by reduced image resolution and anatomical coverage[64,65]. This is due to the under sampling of the MRI k-space in FLASH MRI imaging. This under sampling of data leads to fast imaging at the expense of image resolution and anatomical coverage.

Ideally, a combination of high temporal resolution (fast imaging) – capable to resolve the dynamic first-pass of the contrast agent, full coverage of the lung fields, and high spatial resolution to capture small pulmonary defects would be required for the optimal differential diagnosis of CTED.

Recently, simultaneous multi-slice (SMS) balanced steady state free precession (b-SSFP) imaging has emerged to solve this problem, allowing better anatomical coverage, increased image resolution and accelerated scan time enabling acquisition of multiple slices simultaneously[65,66]. Therefore, it potentially leads to better visualisation of small pulmonary perfusion defects which can be easily missed in case of sub optimal image quality.

SMS b-SSFP has been recently validated for cardiac perfusion imaging where it doubled spatial coverage by acquiring 6 slices at the same time it takes for conventional sequences to acquire 3 slices, while preserving in-plane resolution[65]. The use of SMS b-SSFP for pulmonary perfusion imaging has not been extensively researched, yet further research is warranted considering its promising results for increased anatomical coverage with high image resolution and shorter scan time for cardiac perfusion.

Additionally, pulmonary perfusion MRI involves antero-posterior coronal images covering both lungs and image acquisition on inspiration to minimize respiratory artefacts. To assess perfusion defects, a gadolinium-based MRI contrast injection is used, which offers hyper-intense or hypo-intense signals depending on the amount of blood perfusion in the region of interest over time (dynamic imaging). Recently, free breathing lung MRI was also validated for image quality and reproducibility, showing promise for increased patient comfort during scanning of PH and patients with other lung diseases causing poor breath holding[67,68].

Pulmonary perfusion MRI images can be assessed qualitatively and quantitatively.

Qualitative (visual) assessment of pulmonary perfusion MRI

Current clinical practice is to visually assess the lung perfusion MRI images during the passage of contrast agent through the pulmonary circulation. Dynamic pulmonary perfusion MRI leads to the visualisation of pulmonary arteries' contrast distribution: a pulmonary segment with normal perfusion shows a good and homogeneous perfusion, while the lung territory supplied by a pulmonary artery with partial or complete occlusion due to thromboembolic material will show reduced and delayed perfusion. Impaired lung perfusion can be visually assessed as a wedge-shaped perfusion defect on the pulmonary perfusion images.

However, this observer based qualitative assessment is prone to inter- and intra-observer variations leading to subjective interpretations[69,70].

Quantitative assessment of pulmonary perfusion MRI

To mitigate subjective bias, pulmonary perfusion MRI also allows quantification of perfusion parameters: Pulmonary blood flow, pulmonary blood volume and mean transient time of blood flow (Figures 3 and 4[33,50]) which requires tracing of the contrast agent passing through the tissue of interest and an arterial input function (AIF) curve corresponding to the signal intensity in the blood pool over time[66].

Perfusion quantification is based on the principles of the indicator dilution theory, relating the AIF and tissue enhancement curves *via* the process of deconvolution[71-73], and is often used for the measurement of myocardial blood flow[74]. Pulmonary blood volume (PBV) and mean transit time (MTT) can be subsequently estimated according to the central volume theorem[33,73]. Quantification is, however, significantly impacted by the nonlinear relationship of the

Table 1 Characteristics of included studies

Ref.	Study design	Patients (*n*)	Demographics	Aims	Methodology	Analysis	Results (95%CI)
Amundsen *et al*[31], 1997	Prospective, qualitative	7	7 patients with suspected PE	To evaluate the feasibility of perfusion MRI for detection of perfusion defects distal to suspected pulmonary embolism compared to V/Q	Rapid acquisition of two sets of dynamic images in coronal and trans axial plane	Qualitative analysis (MRI Vs V/Q)	Perfusion MRI correctly identified 16/18 lung segments with perfusion defects
Amundsen *et al*[32], 2002	Prospective, qualitative	42	20 suspected PE, 11 Pneumonias, 11 COPD	To compare perfusion MRI and V/Q for the perfusion defects detection	Rapid acquisition of two sets of dynamic images in coronal and trans axial plane with an inversion recovery gradient MRI sequence	Qualitative analysis (MRI Vs V/Q)	For PE: Intra-modality kappa = 0.77, Inter-observer kappa = 0.92
Ohno *et al*[33], 2004	Prospective, qualitative	40	Controls=15, (Mean age 42 yr), PH patients=25, (Mean age 61 yr)	To assess regional differences in quantitative pulmonary perfusion parameters using MRI	Three dimensional ultrafast DCE-MRI was performed and PBF, PBV & MTT measured by signal intensity time course curve	MATLAB, For PBF, MTT, PBV, Mean, SD, ANOVA, Fisher's PLSD test	PBF, PBV & MTT showed significant differences between normal volunteers and patients with PH ($P < 0.05$)
Nikolaou *et al* [34], 2005	Prospective, qualitative	29	16 females (mean age 54 ± 17 yr), 13 males (Mean age 57 ± 15 yr)	Pulmonary hypertension & CTEPH differen-tiation by perfusion MRI and pulmonary angiography	Turbo fast low angle shot gradient echo MRI sequence was performed by using generalized auto calibrating partially parallel technique or GRAPPA	Student t test for significance, ROC using SPSS software	**ROC:** MRA = 0.85, MRI = 0.82, MRA, MRI combined0.90
Kluge *et al* [35], 2005	Prospective, qualitative	31	15 females, 18 males, (Mean age 59.4 yr) with acute PE	To compare the feasibility of perfusion MRI with CT for follow up examination in acute PE	Contrast enhanced 3-dimensional fast low angle shot or FLASH sequence was used for perfusion MRI and time to peak and peak enhancement was measured	T test for paired samples using SPSS	Follow up examination using MRI were feasible compared to CT for all patients
Kluge *et al* [36], 2006	Prospective, qualitative	41	41 patients with suspected PE	To assess the agreement of perfusion MRI with SPECT for identifying perfusion defects	Contrast enhanced 3-dimensional fast low angle shot or FLASH sequence was used for perfusion MRI	Not given	MRI and SPECT agreement kappa Lobar = 0.98, Segmental = 0.98, Subsegmental = 0.69
Ohno *et al*[37], 2007	Prospective, qualitative	28	Controls=14, (Mean age 34 yr), PH patients=14, (Mean age 41 yr)	To measure diagnostic potential of DCE-MRI for pulmonary hypertension	Three dimensional ultrafast DCE-MRI was performed and PBF, PBV & MTT measured by signal intensity time course curve	MATLAB, For PBF, MTT, PBV, MathWorks, Mean, SD, T test	Difference for study groups: PBF: $P < 0.0001$, PBV: $P < 0.0001$, MTT: $P < 0.0001$
Ley *et al*[38], 2007	Prospective, qualitative	25	Controls=5, PH patients=20	To measure diagnostic potential of DCE-MRI for pulmonary hypertension	Contrast enhanced 3-dimensional fast low angle shot or FLASH sequence was used for perfusion MRI	Quantitative analysis of PBF, PBV and MTT, Mann-Whitney U-test	PBF, PBV & MTT showed significant differences between normal volunteers and patients with PH ($P < 0.05$)
Ohno *et al*[39], 2008	Prospective, qualitative	27	Controls = 9, 18 gender and age matched CTD patients	To measure diagnostic potential of DCE-MRI for PAH	PBF, MTT and PBV measured by DCE-MRI and correlated by %DL(CO) measured by pulmonary function test and mPAP, sPAP measured by doppler echo	MATLAB, MathWorks, Mean, SD, T test, Correlation test	PBF, MTT, PBV correlated positively with %DL(CO) & sPAP ($P < 0.05$), PBF& PBV correlated positively with mPAP& moderately with PVR ($P < 0.05$)
Ohno *et al*[40], 2010	Prospective, qualitative	50	50 PE patients with acute pulmonary thromboembolism (APTE)	To measure diagnostic potential of DCE-MRI for acute pulmonary	PBF, PBV, MTT & APTE index measured by DCE-MRI using 3-dimensional spoiled	ROC curve, Logistic regression	PBF and MTT significantly lower for APTE segments to non-APTE segments (

				thromboembolism (APTE)	gradient sequence, MPAP, PVR measured by RHC. RV/LV diameter ratio, APTE index measured by CT & MRA		$P < 0.05$), APTE indexes from all modalities proved significant predictors for differentiating APTE patients
Stein *et al*[41], 2010	Prospective, qualitative	371	371 adults with diagnosed or excluded pulmonary embolism- (PIOPED III)	To assess performance of MRA and venography for pulmonary embolism detection	MRA was compared with CTPA, V/Q scan, venous ultrasonography, D-dimer assay, and clinical assessment, Qualitative assessment by expert reader only	Chi-square test ANOVA	Technically adequate images for MRA: SE: 78%, SP: 99%
Kang *et al*[42], 2011	Prospective, qualitative	35	35 PAH patients (Mean age 44 yr)	To assess if Cardiac MRI based pulmonary artery distensibility index correlates with RHC estimates for PAH	Pulmonary artery distensibility indices were derived from transverse view MRI and compared with PVR using RHC	Correlation	Non-invasive MRI based pulmonary artery distensibility index correlates with RHC based estimates $P < 0.001$
Ohno *et al*[43], 2012	Prospective, qualitative	24	Response group=13, Non-response group=11, 12 females & 12 males mean age 68 yr ± 8.6	CTPA, MRA & DCE-MRI comparison for treatment response in inoperable CTEPH patients	PBF, PBV, MTT measured by DCE-MRI using 3-dimensional spoiled gradient sequence, RV/LV diameter ratio and embolic burden measured by CTPA & MRA	Mean of student T test, Correlation, ROC curve analysis, McNemar's test	DCE-MRI SP = 90%, AC = 95%, CTPA SP = 36%, AC = 70%, MRA SP = 54%, AC = 79%
Ley *et al*[44], 2013	Prospective, qualitative	20 PAH or CTEPH patients	Controls 10, Training group 10	To evaluate if training improves pulmonary perfusion in PH as assessed by MR perfusion imaging	Training group received in hospital exercise training while control group received conventional rehabilitation. 6 min walk test, PBF, PBV, MTT & peak flow velocity measured by MR perfusion were assessed for both groups from baseline to 3 wk	Mann-Whitney-Wilcoxon test, Spearman correlation coefficient	Training group had significantly improved 6-min walk test, MR flow and MR perfusion
Rajaram *et al* [45], 2013	Prospective, qualitative	132	78 CTEPH patients	To compare the diagnostic accuracy of perfusion MRI for CTEPH Vs. CTPA and V/Q	Pulmonary perfusion MRI using time resolved 3-Dimensional spoiled gradient and pulmonary MRA were compared with CTPA and V/Q	Not given	SE, SP in %, MRI: 97, 92, V/Q: 96, 90, CTPA: 94, 98
Revel *et al*[46], 2013	Prospective, qualitative	274	274 suspected PE patients	To evaluate unenhanced, enhanced perfusion and MR angiography for PE detection	Unenhanced steady state free precession or SSFP, fast spoiled gradient echo for perfusion MRI and MR angiography were compared with CTPA	Chi-squared Kappa statistics	Kappa agreement MRA = 0.77, Perfusion MRI = 0.51, Unenhanced MRI = 0.62
Sugimoto *et al* [47], 2013	Prospective, qualitative	34	34 congenital heart disease patients	To assess if velocity encoded cine imaging can measure pulmonary artery pressure in children with congenital heart disease	Pulmonary blood flow (QP), systemic blood flow (QS), acceleration time, ejection time, peak velocity, and maximal change in flow rate during ejection (MCFR) were measured by velocity encoded MRI and RHC		Velocity encoded MRI correlated strongly with RHC for QS, right to left QP ratio and QP/QS. Suggesting usefulness of MRI for pulmonary artery pressure measurement
Schoenfeld *et al*[48], 2015	Prospective, qualitative	64	64 ruled out or confirmed PE patients	To compare perfusion weighted Fourier decomposition or PW-FD to DCE-MRI for PE detection	Time resolved angiography with stochastic trajectories or TWIST for DCE-MRI was used and compared with PW-FD	Qualitative only, Kappa statistics	For PW-FD per patient basis, SE = 100%, SP = 95%, PPV = 98%, NPV = 98%, Intraobserver k = 0.96, Interobserver k = 0.96
Ingrisch *et al* [49], 2016	Prospective, qualitative	18	8 acute PE, 10 controls	DCE-MRI evaluation for acute PE	Qualitative assessment of presence and	Cohen's kappa, Fisher's	SE: 87-93%, SP: 90-95%, PPV: 87-93%,

				detection compared with CTPA	absence of perfusion defects using DCE-MRI using TWIST sequence	exact test	NPV: 90-95%, Inter-reader agreement: k = 0.77, Intra-modality agreement: $P < 0.001$
Johns *et al*[50], 2017	Prospective, qualitative	74	20 male, 26 female, Mean age 62 ± 14 yr	DCE-MRI, SPECT & CTPA comparison for CTEPH diagnosis	Qualitative comparison of presence/absence of perfusion defects on DCE-MRI using fast spoiled gradient echo, perfusion, SPECT and CTPA	2*2 predictive table, Kappa (k) for inter-observer agreement	SE: 100%, SP: 81%, PPV: 90%, NPV: 100%, Inter-observer agreement for DCE-MRI: k = 0.88, SPECT: (k = 0.80)
Voskrebenzev *et al*[51], 2018	Prospective, qualitative	5	2 controls, 1 CTEPH patient 1 CF patient, 1 obstructive pulmonary disease patient	To assess the feasibility of phase resolved functional lung MRI (PREFUL) for quantitative reginal ventilation and perfusion	Time to peak, V/Q maps and fractional ventilation flow volume were calculated using PREFUL MRI	Full Cardiac and respiratory cycle were sorted using PREFUL	Post endarterectomy, CTEPH patient showed increased perfusion time to peak in visual agreement with DCE-MRI
Agoston-Coldea *et al* [52], 2018	Prospective, qualitative	30	30 consecutive patients with COPD and suspected secondary pulmonary hypertension	To evaluate ability of CMR right ventricular parameters and pulmonary artery stiffness to identify pulmonary hypertension	Clinical examination. 6-min walk test, echocardiography, RHC and cardiac functions and late gadolinium CMR imaging with phase contrast flow imaging of pulmonary artery. Followed up for a mean period of 16 mo	ROC curve analysis, Kolmogorov-Smirnov test, ANOVA test. Fischer's exact test	Pulse wave velocity: SE = 93.5%, SP = 92.8%
Schoenfeld *et al*[53], 2019	Prospective, qualitative	29	20 CTEPH patients	Cardiopulmonary evaluation of treatment response after BPA in CTEPH patients	PBF and first pass bolus kinetic parameters and biventricular mass and functions were evaluated using MRI	Paired two sides Wilcoxon rank sum test, Spearman p correlation, Multiple linear regression	Post BPA, PBF changes in treated lobes were significantly higher than non-treated lobes $P < 0.05$, MRI derived pulmonary artery pressure ejection fraction, RV stroke volume, CO, ventricular mass index & PBF in non-treated lobes correlated with PBF changes in treated lobes $P < 0.05$
Ray *et al*[54], 2019	Prospective, qualitative	51	20 mild PH, 31 moderate to severe PAH	Utility of pulmonary artery pulsatility by cardiac MRI as an early marker of pulmonary hypertension	Standards steady state free precession or cine SSFP for pulmonary artery pulsatility and phased contrast MRI imaging for pulmonary flow assessment	Wilcoxon rank sum test, Roc analysis	Pulmonary artery pulsatility declined from normal (53%), mild (22%) and moderate to severe PAH (17%)
Alsady *et al* [55], 2021	Prospective, qualitative	20	20 CTEPH patients	To compare DCE-MRI and computed tomography for lung perfusion defects before and after pulmonary endarterectomy	Lobe based analysis of perfusion defects using DCE-MRI and PBF and PBV measurement, comparison with dual energy computed tomography	Pearson product-moment correlation, Paired t test using MATLAB	Correlation between CT and MRI based perfusion defects ($r > 0.78$; $P < 0.001$)
Torres *et al* [56], 2022	Prospective, qualitative	41	20 IPF patients	DCE-MRI for the evaluation of lung perfusion in IPF	PBF CV, FVC% predicted %DL(CO) and LCI% were evaluated using DCE-MRI	Regression analysis, Spearman rank correlation	DCE-MRI identified regional perfusion defects between controls and IPF ($P < 0.05$). Correlation observed between PBF CV and %DL(CO) ($r = 0.48$, $P < 0.001$)

AC: Diagnostic accuracy; APTE: Acute pulmonary thromboembolism; BPA: Balloon pulmonary angioplasty; CI: Confidence interval; COPD: Chronic obstructive pulmonary disease; CTEPH: Chronic thromboembolic pulmonary hypertension; CTPA: computed tomography pulmonary angiography; CO: Cardiac output; CV: Coefficient of variation; DCE-MRI: Dynamic contrast enhanced magnetic resonance imaging; %DL(CO): Diffusing capacity of carbon monoxide; LV: Left ventricle; LCI: %(lung clearance index), MRA: Magnetic resonance angiography; MTT: Mean transit time; NPV: Negative predictive value; PAP: pulmonary artery pressure; PBF: Pulmonary blood flow; PBV: Pulmonary blood volume; PE: Pulmonary embolism; FVC: % Percent predicted

forced vital capacity; PPV: positive predictive value; PVR: Pulmonary venous resistance; ROC: Receiver operating curve; SE: Sensitivity; SP: Specificity; sPAP: Systolic pulmonary artery pressure; SPECT: Single photon emission Computed tomography; SPSS: Statistical package for social sciences; RV: Right ventricle; V/Q: Ventilation perfusion scan.

measured signal with contrast agent concentration leading to errors in quantitative metrics.

Non-linearity is caused by spatial signal variations due to variations in sensitivity profiles of MRI surface coils, contrast bolus related T2* decay and subsequent signal loss[66]. To mitigate this effect, a dual-contrast bolus approach can be used, where a dilute (low concentration) bolus is injected for AIF measurement and a neat (high concentration) bolus is subsequently injected for signal intensity measurement in the lung tissue[75]. Researchers reported that the dual-bolus approach is feasible for pulmonary perfusion MRI, reducing the inherent nonlinearity between contrast concentration and signal intensity[76].

Recently, the dual-sequence approach was introduced to avoid the complexity of injector set up and issues of non-linearity for cardiac perfusion MRI[77]. The dual-sequence approach is more practical in busy clinical settings, as it involves injection of a single contrast bolus. The sequence acquires a low resolution slice by FLASH readout for sampling the AIF, followed by acquisition of high resolution short-axis slices using SSFP or FLASH readout[78]. This dual-sequence technique has been validated for cardiac perfusion imaging for its linearity for signal conversion to contrast bolus concentration[66].

Clinically, MRI perfusion quantification permits user-independence quantification of PBF, PBV and MTT at the global, lobar, and segmental pulmonary levels, minimising inter- and intra-observer qualitative bias[69]. Quantification of perfusion parameters allow narrowing down the differential diagnosis of lesions associated with increased or decreased PBF or PBV, (as in the case of chronic thromboembolic partial or complete obstruction of pulmonary vasculature[79].

Diagnostic accuracy of pulmonary perfusion in the literature

Evaluation of pulmonary thromboembolic disease by lung perfusion MRI is a relatively new imaging technique, and its diagnostic potential has been reported comparable with the routinely performed tests of CTPA and SPECT scintigraphy [43,50,63]. The diagnostic accuracy of pulmonary perfusion has been tested qualitatively and quantitatively.

Qualitative assessment: An early feasibility study looking at the diagnostic accuracy of perfusion MRI for detecting lung perfusion defects in patients with pulmonary embolism revealed a good inter-modality agreement with V/Q scan by correctly identifying 16 out of 18 perfusion defects[31].

The diagnostic accuracy of pulmonary perfusion MRI has been demonstrated comparable to V/Q scan measured by the Kappa statistic (k) for inter-observer and inter-modality agreement (inter-observer agreement: k = 0.63 and inter-modality agreement: k = 0.79) in another prospective qualitative study assessing the treatment response of inoperable CTEPH patients[34].

A prospective qualitative study on 78 CTEPH patients assessing the diagnostic accuracy of pulmonary perfusion MRI concluded a sensitivity of 97% and specificity of 92% compared to V/Q and CTPA[45]. Another qualitative comparison for evaluating the diagnostic potential of pulmonary perfusion MRI for the detection of pulmonary embolism reported a sensitivity of 87%-93% and a specificity of 90%-95% with an inter-observer agreement of k = 0.77[49]. Similarly, another study prospectively comparing the diagnostic potential of perfusion MRI, perfusion SPECT and CTPA revealed sensitivity 100% and specificity 81% with inter-observer agreement of k=0.88 for perfusion MRI compared to inter-observer agreement of k = 0.80 ($P < 0.0001$) for SPECT scintigraphy[50].

Quantitative assessment: Prospective quantitative studies affirm the diagnostic potential of pulmonary perfusion MRI by measuring the perfusion parameters of PBF, PBV and MTT for normal, CTEPH and PH of other aetiologies leading to early differential diagnosis and better disease management[37,39,40,43].

Pulmonary perfusion parameters of PBF, PBV and MTT for healthy volunteers and PH patients were quantitatively assessed in a prospective study. Pulmonary perfusion parameters were significantly lower for PH patients accurately differentiating the two study groups[33]. Furthermore, pulmonary perfusion MRI diagnostic accuracy was confirmed in another relevant study where significant results were reported for all three pulmonary perfusion MRI parameters correctly differentiating the two study groups and aiding the differential diagnosis of primary pulmonary hypertension [37].

Additionally, the capability of pulmonary perfusion MRI for the evaluation of disease severity and progression of PAH was compared with pulmonary function test and Doppler echocardiography. Pulmonary perfusion MRI was positively correlated with diffusing capacity of carbon monoxide %DL(CO) measured by pulmonary function test. In the same study, pulmonary perfusion MRI parameters of PBF, PBV and MTT were also positively correlated with mean pulmonary artery pressure and systolic pulmonary artery pressure measured by Doppler echocardiography[39]. This significant correlation implies promising diagnostic potential of pulmonary perfusion MRI for detecting PAH when compared to routine tests.

In another quantitative prospective study, specificity and accuracy of pulmonary perfusion MRI were compared with MDCT and magnetic resonance angiography (MRA) for PH diagnosis. Specificity and accuracy were significantly higher for pulmonary perfusion MRI when right ventricle/Left ventricle diameter ratio and acute pulmonary thromboembolic indices were compared for perfusion MRI, MDCT and MRA ($P < 0.05$). This implies comparable diagnostic capability for pulmonary perfusion MRI to routine tests for PH diagnosis. In this study, PBF was reported as a more accurate perfusion MRI parameter than PBV and MTT[40].

Table 2 Population (P), Intervention (I), Comparison (C), and Outcomes (O) model

PICO	
Population	Pulmonary hypertension patients
Intervention	Cardio-pulmonary MRI, DCE-MRI and/or MRA and/or PREFUL Imaging
Comparator	Computed tomography pulmonary angiography (CTPA) and/or ventilation perfusion (V/Q) scan
Outcome	Diagnostic accuracy
Time frame	1997-2022
Study type	Original retrospective or prospective studies and randomised controlled trials only

MRI: Magnetic resonance imaging; DCE-MRI: Dynamic-contrast enhanced MRI; MRA: Magnetic resonance angiography; PREFUL: Phase resolved functional lung imaging.

Table 3 Inclusion and exclusion criteria for study selection

Inclusion criteria	Exclusion criteria	Rationale
All publication to date	N/A	To avoid missing any relevant studies
English articles	Articles not translated into English	Difficult comprehension
Known or suspected PH patients	Other pulmonary conditions	Pulmonary hypertension is the focus of the study
Original research Prospective/Retrospective only	Reviews, meta-analyses, and case reports	Complicates the results Irrelevant study designs
Papers discussing diagnostic accuracy of MRI, CTPA and V/Q scan	Papers discussing diagnostic accuracy of gas exchange and other techniques	Irrelevant for current study focus

CTPA: Computed tomography pulmonary angiography; MRI: Magnetic resonance imaging; N/A: Not applicable; PH: Pulmonary hypertension.

Table 4 Facet analysis and search strategy

Electronic database	Search string
PubMed	("Pulmonary hypertension" OR "Pulmonary arterial hypertension" OR "Chronic Thromboembolic Pulmonary Hypertension" OR "Left heart pulmonary hypertension" OR "Lung disease pulmonary hypertension" OR "Pulmonary veno-occulusive disease") AND ("Magnetic Resonance Imaging" OR "Pulmonary perfusion Magnetic Resonance Imaging" OR "Cardiac Magnetic Resonance Imaging" OR "Magnetic resonance angiography" OR "Phase resolved functional " OR "Dynamic Contrast Enhanced-Magnetic Resonance Imaging" OR "3Dimensional Dynamic Contrast Enhanced-Magnetic Resonance Imaging" AND ("Computed Tomography pulmonary angiography" OR Ventilation/perfusion scan") AND ("Specificity" OR "Sensitivity" OR "Diagnostic accuracy" OR "Positive predictive value" OR "Area under the curve" OR "screening accuracy")
EMBASE	("Pulmonary hypertension" OR "Pulmonary arterial hypertension" OR "Chronic Thromboembolic Pulmonary Hypertension" OR "Left heart pulmonary hypertension" OR "Lung disease pulmonary hypertension" OR "Pulmonary veno-occulusive disease") AND ("Magnetic Resonance Imaging" OR "Pulmonary perfusion Magnetic Resonance Imaging" OR "Cardiac Magnetic Resonance Imaging" OR "Magnetic resonance angiography" OR "Phase resolved functional " OR "Dynamic Contrast Enhanced-Magnetic Resonance Imaging" OR "3Dimensional Dynamic Contrast Enhanced-Magnetic Resonance Imaging" AND ("Computed Tomography pulmonary angiography" OR Ventilation/perfusion scan") AND ("Specificity" OR "Sensitivity" OR "Diagnostic accuracy" OR "Positive predictive value" OR "Area under the curve" OR "screening accuracy")
Medline	("Pulmonary hypertension" OR "Pulmonary arterial hypertension" OR "Chronic Thromboembolic Pulmonary Hypertension" OR "Left heart pulmonary hypertension" OR "Lung disease pulmonary hypertension" OR "Pulmonary veno-occulusive disease") AND ("Magnetic Resonance Imaging" OR "Pulmonary perfusion Magnetic Resonance Imaging" OR "Cardiac Magnetic Resonance Imaging" OR "Magnetic resonance angiography" OR "Phase resolved functional " OR "Dynamic Contrast Enhanced-Magnetic Resonance Imaging" OR "3Dimensional Dynamic Contrast Enhanced-Magnetic Resonance Imaging" AND ("Computed Tomography pulmonary angiography" OR Ventilation/perfusion scan") AND ("Specificity" OR "Sensitivity" OR "Diagnostic accuracy" OR "Positive predictive value" OR "Area under the curve" OR "screening accuracy")

Moreover, researchers compared the accuracy of treatment response in inoperable CTEPH patients using pulmonary perfusion MRI, CTPA and MRA. This comparative prospective study found higher diagnostic accuracy (95%) and specificity (90%) for pulmonary perfusion MRI compared to CTPA to differentiate treatment responders and non-responders[43]. A recent quantitative study assessed the regional PBF pre and post PEA using pulmonary perfusion MRI and compared it with exercise capacity post PEA for CTEPH patient. They concluded a positive correlation between perfusion MRI for identifying improvement in PBF in the lower lungs and exercise capacity after successful surgery[80].

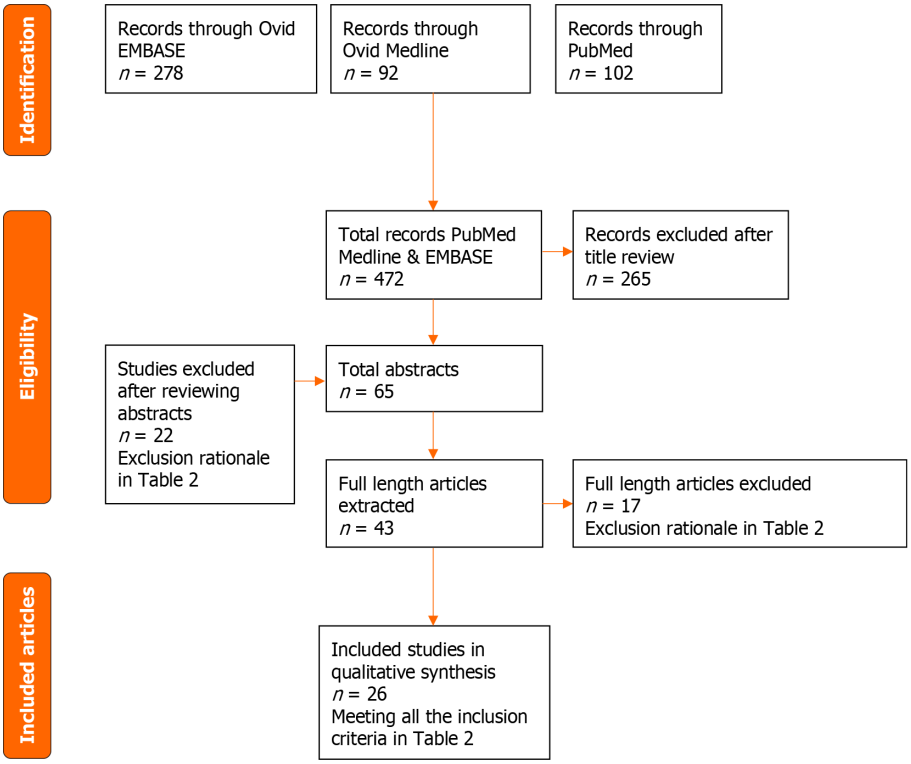

DOI: 10.4329/wjr.v15.i9.256

Figure 1 PRISMA flow chart for literature search.

This literature search concludes the approving potential of pulmonary perfusion MRI for the differential diagnosis of PH. However, most of these comparative studies were single centre with small sample size, therefore further large-scale multicentre research is recommended.

Hyperpolarised inhaled contrast agent pulmonary MRI

Hyperpolarised gases like ^{3}He, ^{129}Xe and Oxygen-enhanced ^{1}H have also gained popularity for assessing pulmonary ventilation and perfusion in lung diseases. A retrospective study on 15 patients was conducted to assess regional lung ventilation as part of pre-operative planning of lobectomy, pneumonectomy or lung volume reduction surgery. This study reported good agreement between ^{3}He MRI and scintigraphy ventilation imaging to diagnose ventilation defects [81]. Another case study of CTEPH patient demonstrated the use of ^{3}He ventilation scan combined with dynamic contrast enhanced perfusion MRI to assess the treatment response of pre and post PEA[82].

^{129}Xe is of particular interest for CTEPH diagnosis because ^{129}Xe has an ability to dissolve in pulmonary tissues. After inhalation, ^{129}Xe is easily soluble in lung tissues and blood leading to frequency shift which can be quantitatively measured by MR spectroscopy[83]. ^{129}Xe has been tested to demonstrate a reduced uptake of red blood cells in CTEPH and pulmonary vascular disease patients indicating perfusion defects[84,85]. Another study on 10 PAH patients, ^{129}Xe MRI showed reduced RBC amplitude oscillations on MRI spectroscopy implying its potential to diagnose pulmonary vascular diseases from other lung disorders[86]. These initial results reflect the potential of combining hyperpolarised gas MRI imaging with cardiopulmonary MRI to comprehensively assess the structural and functional ventilation and perfusion pulmonary disorders.

However, hyperpolarised inhaled contrast agent pulmonary MRI is still an emerging modality and further large-scale research is needed to strengthen its diagnostic potential to conventional perfusion scintigraphy.

Advantages of pulmonary perfusion MRI

Ionising radiation free diagnostic test: Screening and follow-up scans to monitor the disease progression is a crucial part of management strategy for patients with PH. In a prospective longitudinal study in a cohort of 675 emergency department patients researchers concluded that at least one third of patients undergoing CTPA were called for a follow up scan within 5 years, with one fifth of patients being women younger than 40 years old[21]. In addition, it is estimated that 5% to 11% of CTPA scans for the diagnosis of CTEPH are repeated due to artefacts and technical reasons, which further exacerbate the risk of excessive radiation dose in another study[87]. This unnecessary ionising radiation exposure can be reduced by using pulmonary perfusion MRI at screening and diagnostic stages of CTEPH leading to better patient healthcare strategy.

An all-inclusive test: Besides lung perfusion imaging, the cardiac assessment is also important in patients with PH. Cardiac involvement in PH is an inevitable step in the disease progression and PH due to left heart disease is the most common type[88,89]. It is reported that more than half of heart failure patients suffer from PH[90]. The pressure increase

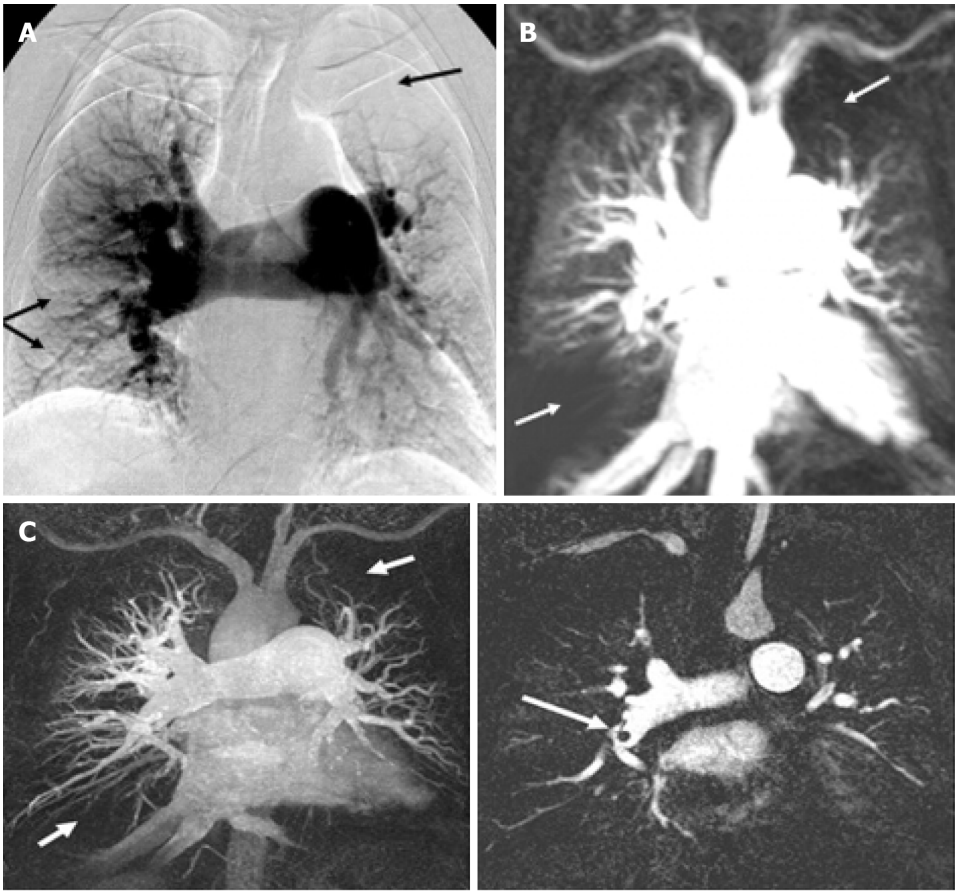

Figure 2 Comparing digital subtraction angiography, pulmonary perfusion magnetic resonance imaging and magnetic resonance angiography for identifying perfusion defects in chronic thromboembolic pulmonary hypertension patient. A: Digital subtraction angiography showing perfusion defects (arrows) in left upper lobe and right lower lobe due to thromboembolic occlusion; B: Magnetic resonance imaging perfusion image at peak enhancement showing hypo-intense perfusion defects at same locations; C: Magnetic resonance angiogram of the same patient demonstrating dark thromboembolic material in the right pulmonary artery corresponding to perfusion defects at the same location. Citation: Nikolaou K, Schoenberg SO, Attenberger U, Scheidler J, Dietrich O, Kuehn B, Rosa F, Huber A, Leuchte H, Baumgartner R, Behr J, Reiser MF. Pulmonary arterial hypertension: diagnosis with fast perfusion MR imaging and high-spatial-resolution MR angiography--preliminary experience. *Radiology 2005*; 236: 694-703 [PMID: 15994997 DOI: 10.1148/radiol.2361040502].

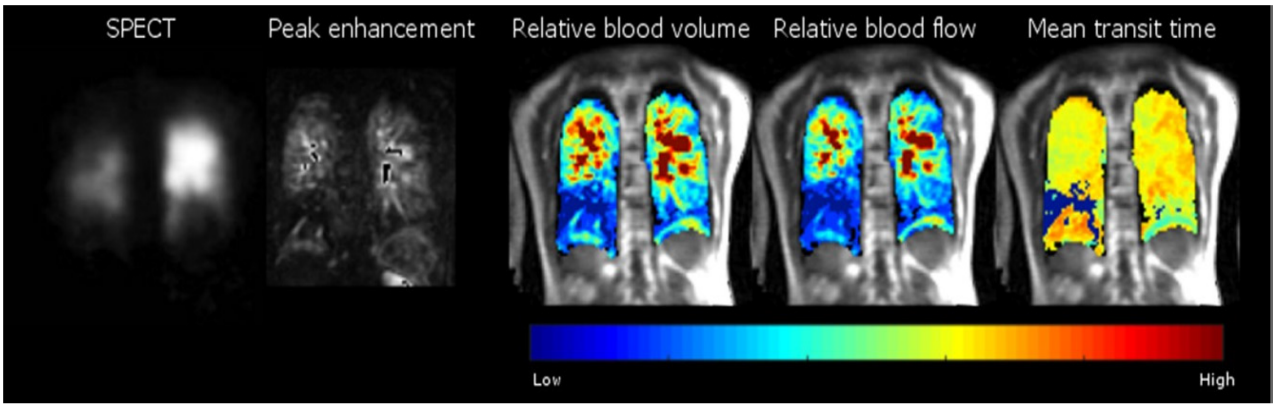

Figure 3 Comparing single photon emission computed tomography and dynamic contract enhanced perfusion magnetic resonance imaging for identifying perfusion defects in chronic thromboembolic pulmonary hypertension patient. Left to right, single photon emission computed tomography and Perfusion magnetic resonance imaging (MRI) at peak enhancement of a chronic thromboembolic pulmonary hypertension patient showing perfusion defects in right and left lower lobes. On the right, semi-quantitative pulmonary blood flow, pulmonary blood volume & mean transit time maps acquired from perfusion MRI demonstrating reduced flow at the same locations. Note left to right scale depicting lower to higher pulmonary blood flow values. Citation: Johns CS, Swift AJ, Rajaram S, Hughes PJC, Capener DJ, Kiely DG, Wild JM. Lung perfusion: MRI vs. SPECT for screening in suspected chronic thromboembolic pulmonary hypertension. *J Magn Reson Imaging* 2017; 46: 1693-1697 [PMID: 28376242 DOI: 10.1002/jmri.25714].

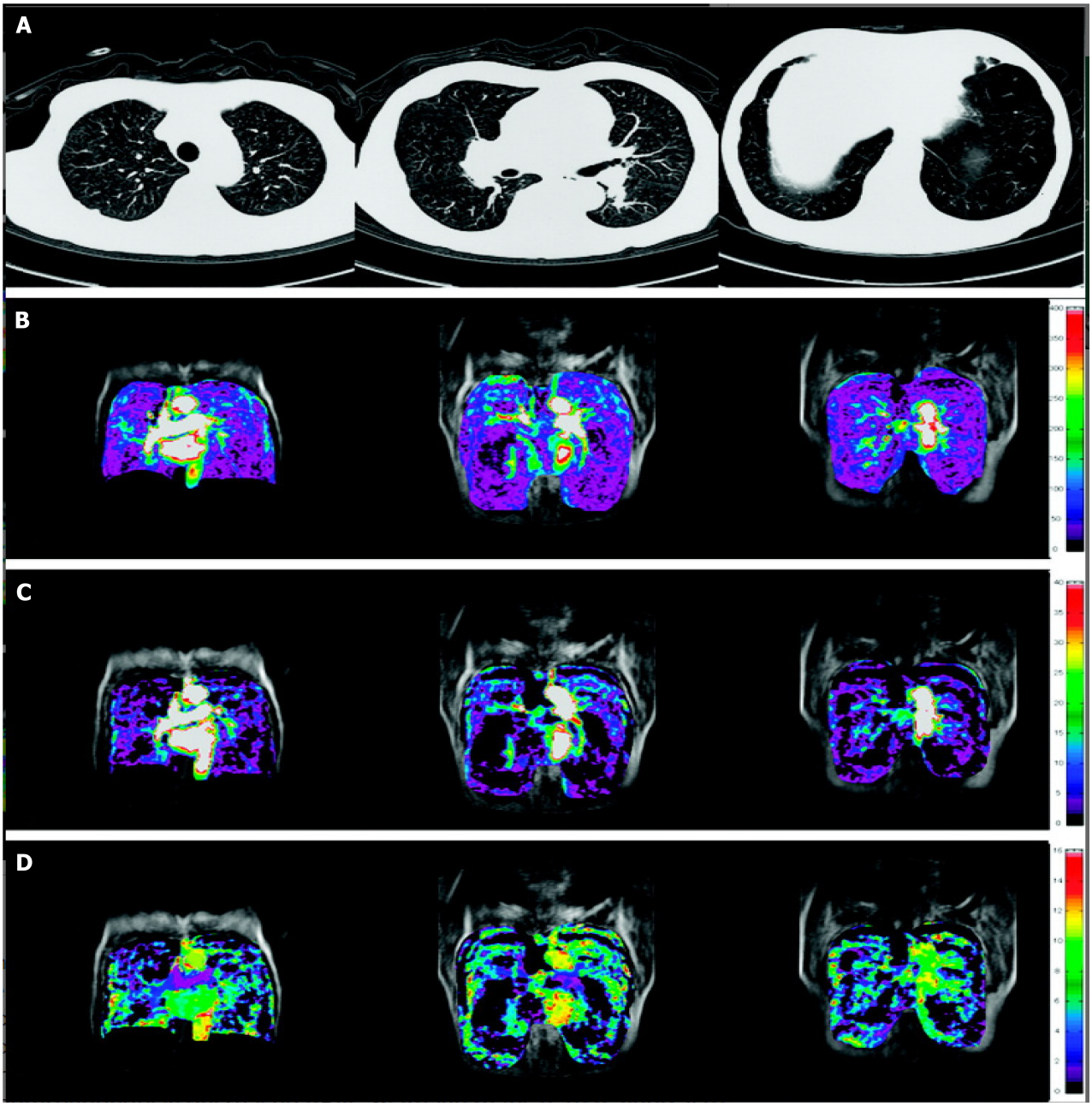

Figure 4 Comparing computed tomography chest and dynamic contract enhanced perfusion magnetic resonance imaging for identifying perfusion defects in pulmonary hypertension patient with COPD. A: Chest computed tomography showing lobular emphysema in the lungs; B-D: Quantitative perfusion maps (anterior to posterior) showing heterogeneously reduced pulmonary blood flow, pulmonary blood volume and mean transit time respectively representing thromboembolic occlusion in respective pulmonary segments. Note on the right-hand side, quantitative scale from top to bottom showing higher to lower quantitative values. Citation: Ohno Y, Hatabu H, Murase K, Higashino T, Kawamitsu H, Watanabe H, Takenaka D, Fujii M, Sugimura K. Quantitative assessment of regional pulmonary perfusion in the entire lung using three-dimensional ultrafast dynamic contrast-enhanced magnetic resonance imaging: Preliminary experience in 40 subjects. *J Magn Reson Imaging* 2004; 20: 353-365 [PMID: 15332240 DOI: 10.1002/jmri.20137].

in the pulmonary arteries leads to an increase in the RV pressure and cardiac remodelling, correlated with increased mortality. RV end-systolic volume index has been reported as an independent predictor of PAH prognosis in a study using 288 derivation cohort and 288 validation PAH cohort[91].

Moreover, another relevant study validated that cardiac MRI based pulmonary artery distensibility index correlates positively with the right heart catheterization estimates for PAH, suggesting non-invasive cardiac MRI a valuable tool for PAH diagnosis[42].

Additionally, cardiac magnetic resonance imaging has also been used to assess pulmonary artery pressure measurements in children with congenital heart disease. Researchers found velocity encoded flow cardiac MRI images strongly correlated with right heart catheterization for systemic blood flow (QS), right to left pulmonary blood flow (QP) ratio and QP/QS ratio[47]. This suggests usefulness of cardiac MRI for pulmonary artery pressure measurement by using the standard SSFP cine imaging and phase contrast flow imaging.

Pulmonary perfusion can be combined with cardiac MRI, including cardiac cine images for structural and functional assessment of heart chambers, blood flow assessment by phase contrast imaging, MRA, post contrast late gadolinium enhancement imaging for myocardial fibrosis/scarring and four-dimensional phase contrast pulmonary artery flow scan. A comprehensive cardio-pulmonary assessment can be achieved in a single examination during the same visit, leading to better use of health resources and limiting the patients' stress[83].

Quantification mitigates observer bias: MRI pulmonary perfusion offers quantification of PBF, PBV and MTT with improved diagnostic accuracy. In a study assessing the diagnostic accuracy of qualitative and quantitative cardiac MR perfusion in coronary artery disease, the level of training was reported as a major determinant for the accuracy of qualitative assessment (the diagnostic accuracy of level-3 operators was 83.6%, level-2 operators 65.7% and level-1 operators 55.7%, $P < 0.001$), while the diagnostic accuracy of quantitative assessment was 86.3% (significantly higher than level-2 and level-1 operators), highlighting the usefulness of operator-independent quantification techniques[70].

Moreover, higher consistency and reproducibility results were achieved using quantification techniques, and an increased sensitivity (from 77% to 83%) was reported when using quantitative measures for the evaluation of myocardial perfusion[92]. Researchers also studied MRI signal abnormalities in the brain and reported higher reproducibility and accuracy of quantification techniques compared to qualitative analysis by expert radiologists[93]. The quantification of MRI perfusion parameters mitigates this observer bias, which is not achievable with current tests to diagnose PH.

Contrast nephrotoxicity comparison

CT scan uses iodine-containing contrast media which can unfortunately cause serious complications, such as contrast induced nephropathy. Gadolinium-based contrast agents are considered safer than iodinated contrast media, thus they can be safely used also in patients with impaired kidney function[94]. CT contrast also involves a huge dose and contrast related discomfort has also been reported. Additionally, the iodine-based contrast can potentially worsen the thyroid function, on the other hand gadolinium based MRI contrast agents have been reported safer for pregnant patients and patients with compromised renal functions[95]. Some other contraindications for CT contrast injection include multiple myeloma and metformin.

CONSIDERATIONS REGARDING PULMONARY PERFUSION MRI

Claustrophobia and magnet safety related issues

An MRI scanner is a long, tunnel-like enclosed chamber where patients need to lie down still for a long time (minimum 40 min). Patients are further fastened by the radiofrequency coil placed on the chest. The MRI scanner also produces loud banging noise (110 decibels at its loudest)[96]. Lying down still for a long time in such an enclosed chamber and tolerating the loud noise can be challenging for claustrophobic patients or patients with hearing problems. Magnet related safety for medical devices' including cardiac pacemakers, aneurysmal clips, intra orbital metallic injury and some other incompatible metallic implants are some other limitations of MRI scanning.

Consideration about image resolution, scan time and respiratory artefacts

In comparison to computed tomography, MRI is prone to breathing artefacts and it inherently retains low image resolution for moving organs like heart and lungs. Scan time is another limitation for MRI, longer scan time leads to patient discomfort. To mitigate, advanced motion correction techniques of parallel imaging, patient training for breath hold, respiratory/ electrocardiogram gating for cardiac MRI and saturation band to supress signal from moving chest wall and heart motion have been adapted[97].

Moreover, recently researchers have successfully validated free breathing, real time MRI imaging with short scan time and high image resolution for cardiac perfusion imaging[98,99]. More research is warranted to apply this technique for pulmonary perfusion

Technical challenges of pulmonary perfusion quantification

Pulmonary perfusion quantification is technically challenging. It needs a skilled operator and availability of a specific software package for quantification. Furthermore, it is prone to errors when images have respiratory and motion artefacts. Lack of integration with other clinical findings while quantification is another limitation.

Future directions

The Fleischner Society's position paper recommends MRI for clinical use for cystic fibrosis, lung cancer staging, lung nodule characterisation and pulmonary hypertension. The position paper endorses further investigating the role of perfusion MRI for the diagnosis of chronic obstructive pulmonary disease and pulmonary parenchymal abnormalities in future[57]. However, MRI imaging for lungs is still limited in clinical and research fields implying the need for further clinically implementable research in this field[57,100]. An ongoing prospective, multicentre, comparative phase III clinical trial (Change-MRI) is currently being carried out to compare the diagnostic accuracy of perfusion MRI and SPECT scintigraphy for CTEPH diagnosis[101]. Pulmonary perfusion MRI has clinical and technical aspects to be considered for future research on this topic.

Clinically, combining cardiac magnetic resonance with pulmonary perfusion imaging can help differentiate lung disorders of multiple aetiologies. 4-dimentional flow MRI imaging to assess pulmonary artery pressure has been demonstrated to aid CTEPH diagnosis[53,102,103]. Moreover, as SMS b-SSFP MRI sequence has been validated for better

anatomical coverage and improved resolution for cardiac imaging, its use can be expanded for pulmonary perfusion imaging and specifically thromboembolic vascular lung disorders. Additionally, sophisticated software to quantitatively analyse perfusion parameters can further improve diagnostic accuracy in future[57].

Quantitative analysis of perfusion MRI parameters of PBF, PBV and MTT can be performed manually or automatically. Manual quantification can be time consuming and laborious. To improve efficiency, researchers established the validity of automated quantitative analysis for myocardial perfusion MRI and found it more efficient and reproducible than manual analysis[104-106].

Similarly, the automatic analysis of lung MRI has also been researched using artificial intelligence (AI) and deep learning algorithms for automatic lung segmentation of 20 cystic fibrosis patients. This study found automatic lung segmentation comparable with manual segmentation and capable of accurate estimation of lung volume[107]. Researchers also used AI techniques to automatically quantify the neonatal lung structure and compared it with manual segmentation by expert operators. This study found that AI-supported automatic segmentation of lung MRI was accurate and comparable to expert-level accuracy[108]. Therefore, for efficiency of time and consistency of diagnostic parameters, further research on the accuracy of automatic lung segmentation and quantification of perfusion parameters is recommended.

Currently, the dual-bolus approach is preferred in routine clinical practice for perfusion MRI imaging, but the dual-sequence approach to account for signal intensity nonlinearity and operator-friendly set up of injector pump in busy clinical settings is also recommended for future research on this topic[66].

CONCLUSION

PH is multifactorial and requires timely multimodality differential diagnosis for better disease prognosis. Pulmonary perfusion MRI can be considered a reliable and safe diagnostic imaging tool with comparable diagnostic accuracy to reference gold standards of SPECT, CTPA and V/Q imaging. It offers cardiopulmonary assessment when combined with CMR at the same visit without any radiation exposure making it a comprehensive test for screening, differential diagnosis and follow up scans for PH management. Furthermore, quantification of pulmonary perfusion parameters could improve the reliability and accuracy of diagnostic testing and help mitigate subjective interpretation of imaging findings which is not possible by qualitative assessment alone offered by standard tests.

FOOTNOTES

Author contributions: Villa ADM was responsible for the review concept; Lacharie M drafted the manuscript; Lacharie M provided critical revision of the manuscript for important intellectual content; and all authors critically reviewed the content.

Conflict-of-interest statement: Authors declare no conflict of interest for this article.

Country/Territory of origin: United Kingdom

ORCID number: Miriam Lacharie 0000-0002-7282-6894; Adriana Villa 0000-0002-9355-0372; Xenios Milidonis 0000-0002-5446-9459; Amedeo Chiribiri 0000-0003-3394-4289.

Corresponding Author's Membership in Professional Societies: Health and Care Professionalcouncil, RA75559.

S-Editor: Liu JH
L-Editor: A
P-Editor: Zhao S

REFERENCES

1 **Verhoeff K**, Mitchell JR. Cardiopulmonary physiology: why the heart and lungs are inextricably linked. *Adv Physiol Educ* 2017; **41**: 348-353 [PMID: 28679570 DOI: 10.1152/advan.00190.2016]

2 **Maron BA**. Revised Definition of Pulmonary Hypertension and Approach to Management: A Clinical Primer. *J Am Heart Assoc* 2023; **12**: e029024 [PMID: 37026538 DOI: 10.1161/JAHA.122.029024]

3 **Galiè N**, Humbert M, Vachiery JL, Gibbs S, Lang I, Torbicki A, Simonneau G, Peacock A, Vonk Noordegraaf A, Beghetti M, Ghofrani A, Gomez Sanchez MA, Hansmann G, Klepetko W, Lancellotti P, Matucci M, McDonagh T, Pierard LA, Trindade PT, Zompatori M, Hoeper M; ESC Scientific Document Group. 2015 ESC/ERS Guidelines for the diagnosis and treatment of pulmonary hypertension: The Joint Task Force for the Diagnosis and Treatment of Pulmonary Hypertension of the European Society of Cardiology (ESC) and the European Respiratory

Society (ERS): Endorsed by: Association for European Paediatric and Congenital Cardiology (AEPC), International Society for Heart and Lung Transplantation (ISHLT). *Eur Heart J* 2016; **37**: 67-119 [PMID: 26320113 DOI: 10.1093/eurheartj/ehv317]

4 **Kiely DG**, Levin D, Hassoun P, Ivy DD, Jone PN, Bwika J, Kawut SM, Lordan J, Lungu A, Mazurek J, Moledina S, Olschewski H, Peacock A, Puri GD, Rahaghi F, Schafer M, Schiebler M, Screaton N, Tawhai M, Van Beek EJ, Vonk-Noordegraaf A, Vanderpool RR, Wort J, Zhao L, Wild J, Vogel-Claussen J, Swift AJ. EXPRESS: Statement on imaging and pulmonary hypertension from the Pulmonary Vascular Research Institute (PVRI). *Pulm Circ* 2019; **9**: 2045894019841990 [PMID: 30880632 DOI: 10.1177/2045894019841990]

5 **Lan NSH**, Massam BD, Kulkarni SS, Lang CC. Pulmonary Arterial Hypertension: Pathophysiology and Treatment. *Diseases* 2018; **6** [PMID: 29772649 DOI: 10.3390/diseases6020038]

6 **Yaghi S**, Novikov A, Trandafirescu T. Clinical update on pulmonary hypertension. *J Investig Med* 2020; **68**: 821-827 [PMID: 32241822 DOI: 10.1136/jim-2020-001291]

7 **Martinez C**, Wallenhorst C, Teal S, Cohen AT, Peacock AJ. Incidence and risk factors of chronic thromboembolic pulmonary hypertension following venous thromboembolism, a population-based cohort study in England. *Pulm Circ* 2018; **8**: 2045894018791358 [PMID: 29985100 DOI: 10.1177/2045894018791358]

8 **Ohno Y**, Koyama H, Lee HY, Miura S, Yoshikawa T, Sugimura K. Contrast-enhanced CT- and MRI-based perfusion assessment for pulmonary diseases: basics and clinical applications. *Diagn Interv Radiol* 2016; **22**: 407-421 [PMID: 27523813 DOI: 10.5152/dir.2016.16123]

9 **Mortensen J**, Gutte H. SPECT/CT and pulmonary embolism. *Eur J Nucl Med Mol Imaging* 2014; **41** Suppl 1: S81-S90 [PMID: 24213621 DOI: 10.1007/s00259-013-2614-5]

10 **Musch G**, Layfield JD, Harris RS, Melo MF, Winkler T, Callahan RJ, Fischman AJ, Venegas JG. Topographical distribution of pulmonary perfusion and ventilation, assessed by PET in supine and prone humans. *J Appl Physiol (1985)* 2002; **93**: 1841-1851 [PMID: 12381773 DOI: 10.1152/japplphysiol.00223.2002]

11 **Doğan H**, de Roos A, Geleijins J, Huisman MV, Kroft LJ. The role of computed tomography in the diagnosis of acute and chronic pulmonary embolism. *Diagn Interv Radiol* 2015; **21**: 307-316 [PMID: 26133321 DOI: 10.5152/dir.2015.14403]

12 **Soler X**, Hoh CK, Test VJ, Kerr KM, Marsh JJ, Morris TA. Single photon emission computed tomography in chronic thromboembolic pulmonary hypertension. *Respirology* 2011; **16**: 131-137 [PMID: 20920137 DOI: 10.1111/j.1440-1843.2010.01867.x]

13 **Grosse A**, Grosse C, Lang I. Evaluation of the CT imaging findings in patients newly diagnosed with chronic thromboembolic pulmonary hypertension. *PLoS One* 2018; **13**: e0201468 [PMID: 30059549 DOI: 10.1371/journal.pone.0201468]

14 **Remy-Jardin M**, Faivre JB, Pontana F, Molinari F, Tacelli N, Remy J. Thoracic applications of dual energy. *Semin Respir Crit Care Med* 2014; **35**: 64-73 [PMID: 24481760 DOI: 10.1055/s-0033-1363452]

15 **Havránková R**. Biological effects of ionizing radiation. *Cas Lek Cesk* 2020; **159**: 258-260 [PMID: 33445930]

16 **Levine DJ**. Pulmonary arterial hypertension: updates in epidemiology and evaluation of patients. *Am J Manag Care* 2021; **27**: S35-S41 [PMID: 33710842 DOI: 10.37765/ajmc.2021.88609]

17 **Lin EC**. Radiation risk from medical imaging. *Mayo Clin Proc* 2010; **85**: 1142-1146 [PMID: 21123642 DOI: 10.4065/mcp.2010.0260]

18 **Astani SA**, Davis LC, Harkness BA, Supanich MP, Dalal I. Detection of pulmonary embolism during pregnancy: comparing radiation doses of CTPA and pulmonary scintigraphy. *Nucl Med Commun* 2014; **35**: 704-711 [PMID: 24743314 DOI: 10.1097/MNM.0000000000000114]

19 **Bajc M**, Neilly B, Miniati M, Mortensen J, Jonson B. Methodology for ventilation/perfusion SPECT. *Semin Nucl Med* 2010; **40**: 415-425 [PMID: 20920632 DOI: 10.1053/j.semnuclmed.2010.07.002]

20 **Schembri GP**, Miller AE, Smart R. Radiation dosimetry and safety issues in the investigation of pulmonary embolism. *Semin Nucl Med* 2010; **40**: 442-454 [PMID: 20920634 DOI: 10.1053/j.semnuclmed.2010.07.007]

21 **Kline JA**, Courtney DM, Beam DM, King MC, Steuerwald M. Incidence and predictors of repeated computed tomographic pulmonary angiography in emergency department patients. *Ann Emerg Med* 2009; **54**: 41-48 [PMID: 18838194 DOI: 10.1016/j.annemergmed.2008.08.015]

22 **Ray JC**, Burger C, Mergo P, Safford R, Blackshear J, Austin C, Fairweather D, Heckman MG, Zeiger T, Dubin M, Shapiro B. Pulmonary arterial stiffness assessed by cardiovascular magnetic resonance imaging is a predictor of mild pulmonary arterial hypertension. *Int J Cardiovasc Imaging* 2019; **35**: 1881-1892 [PMID: 29934885 DOI: 10.1007/s10554-018-1397-y]

23 **Olsson KM**, Meyer B, Hinrichs J, Vogel-Claussen J, Hoeper MM, Cebotari S. Chronic thromboembolic pulmonary hypertension. *Dtsch Arztebl Int* 2014; **111**: 856-862 [PMID: 25585582 DOI: 10.3238/arztebl.2014.0856]

24 **Riedel M**, Stanek V, Widimsky J, Prerovsky I. Longterm follow-up of patients with pulmonary thromboembolism. Late prognosis and evolution of hemodynamic and respiratory data. *Chest* 1982; **81**: 151-158 [PMID: 7056079 DOI: 10.1378/chest.81.2.151]

25 **Gopalan D**, Delcroix M, Held M. Diagnosis of chronic thromboembolic pulmonary hypertension. *Eur Respir Rev* 2017; **26** [PMID: 28298387 DOI: 10.1183/16000617.0108-2016]

26 **Mayer E**, Jenkins D, Lindner J, D'Armini A, Kloek J, Meyns B, Ilkjaer LB, Klepetko W, Delcroix M, Lang I, Pepke-Zaba J, Simonneau G, Dartevelle P. Surgical management and outcome of patients with chronic thromboembolic pulmonary hypertension: results from an international prospective registry. *J Thorac Cardiovasc Surg* 2011; **141**: 702-710 [PMID: 21335128 DOI: 10.1016/j.jtcvs.2010.11.024]

27 **Madani MM**, Auger WR, Pretorius V, Sakakibara N, Kerr KM, Kim NH, Fedullo PF, Jamieson SW. Pulmonary endarterectomy: recent changes in a single institution's experience of more than 2,700 patients. *Ann Thorac Surg* 2012; **94**: 97-103 [PMID: 22626752 DOI: 10.1016/j.athoracsur.2012.04.004]

28 **Jenkins D**, Mayer E, Screaton N, Madani M. State-of-the-art chronic thromboembolic pulmonary hypertension diagnosis and management. *Eur Respir Rev* 2012; **21**: 32-39 [PMID: 22379172 DOI: 10.1183/09059180.00009211]

29 **Hopkins SR**, Wielpütz MO, Kauczor HU. Imaging lung perfusion. *J Appl Physiol (1985)* 2012; **113**: 328-339 [PMID: 22604884 DOI: 10.1152/japplphysiol.00320.2012]

30 **Aziz M**, Krishnam M, Madhuranthakam AJ, Rajiah P. Update on MR imaging of the pulmonary vasculature. *Int J Cardiovasc Imaging* 2019; **35**: 1483-1497 [PMID: 31030315 DOI: 10.1007/s10554-019-01603-y]

31 **Amundsen T**, Kvaerness J, Jones RA, Waage A, Bjermer L, Nilsen G, Haraldseth O. Pulmonary embolism: detection with MR perfusion imaging of lung--a feasibility study. *Radiology* 1997; **203**: 181-185 [PMID: 9122390 DOI: 10.1148/radiology.203.1.9122390]

32 **Amundsen T**, Torheim G, Kvistad KA, Waage A, Bjermer L, Nordlid KK, Johnsen H, Asberg A, Haraldseth O. Perfusion abnormalities in pulmonary embolism studied with perfusion MRI and ventilation-perfusion scintigraphy: an intra-modality and inter-modality agreement study. *J Magn Reson Imaging* 2002; **15**: 386-394 [PMID: 11948827 DOI: 10.1002/jmri.10092]

33 **Ohno Y**, Hatabu H, Murase K, Higashino T, Kawamitsu H, Watanabe H, Takenaka D, Fujii M, Sugimura K. Quantitative assessment of

regional pulmonary perfusion in the entire lung using three-dimensional ultrafast dynamic contrast-enhanced magnetic resonance imaging: Preliminary experience in 40 subjects. *J Magn Reson Imaging* 2004; **20**: 353-365 [PMID: 15332240 DOI: 10.1002/jmri.20137]

34 **Nikolaou K**, Schoenberg SO, Attenberger U, Scheidler J, Dietrich O, Kuehn B, Rosa F, Huber A, Leuchte H, Baumgartner R, Behr J, Reiser MF. Pulmonary arterial hypertension: diagnosis with fast perfusion MR imaging and high-spatial-resolution MR angiography--preliminary experience. *Radiology* 2005; **236**: 694-703 [PMID: 15994997 DOI: 10.1148/radiol.2361040502]

35 **Kluge A**, Gerriets T, Lange U, Bachman G. MRI for short-term follow-up of acute pulmonary embolism. Assessment of thrombus appearance and pulmonary perfusion: a feasibility study. *Eur Radiol* 2005; **15**: 1969-1977 [PMID: 15891888 DOI: 10.1007/s00330-005-2760-7]

36 **Kluge A**, Gerriets T, Stolz E, Dill T, Mueller KD, Mueller C, Bachmann G. Pulmonary perfusion in acute pulmonary embolism: agreement of MRI and SPECT for lobar, segmental and subsegmental perfusion defects. *Acta Radiol* 2006; **47**: 933-940 [PMID: 17077044 DOI: 10.1080/02841850600885377]

37 **Ohno Y**, Hatabu H, Murase K, Higashino T, Nogami M, Yoshikawa T, Sugimura K. Primary pulmonary hypertension: 3D dynamic perfusion MRI for quantitative analysis of regional pulmonary perfusion. *AJR Am J Roentgenol* 2007; **188**: 48-56 [PMID: 17179345 DOI: 10.2214/AJR.05.0135]

38 **Ley S**, Mereles D, Risse F, Grünig E, Ley-Zaporozhan J, Tecer Z, Puderbach M, Fink C, Kauczor HU. Quantitative 3D pulmonary MR-perfusion in patients with pulmonary arterial hypertension: correlation with invasive pressure measurements. *Eur J Radiol* 2007; **61**: 251-255 [PMID: 17045440 DOI: 10.1016/j.ejrad.2006.08.028]

39 **Ohno Y**, Koyama H, Nogami M, Takenaka D, Matsumoto S, Onishi Y, Matsumoto K, Murase K, Sugimura K. Dynamic perfusion MRI: capability for evaluation of disease severity and progression of pulmonary arterial hypertension in patients with connective tissue disease. *J Magn Reson Imaging* 2008; **28**: 887-899 [PMID: 18821609 DOI: 10.1002/jmri.21550]

40 **Ohno Y**, Koyama H, Matsumoto K, Onishi Y, Nogami M, Takenaka D, Yoshikawa T, Matsumoto S, Sugimura K. Dynamic MR perfusion imaging: capability for quantitative assessment of disease extent and prediction of outcome for patients with acute pulmonary thromboembolism. *J Magn Reson Imaging* 2010; **31**: 1081-1090 [PMID: 20432342 DOI: 10.1002/jmri.22146]

41 **Stein PD**, Chenevert TL, Fowler SE, Goodman LR, Gottschalk A, Hales CA, Hull RD, Jablonski KA, Leeper KV Jr, Naidich DP, Sak DJ, Sostman HD, Tapson VF, Weg JG, Woodard PK; PIOPED III (Prospective Investigation of Pulmonary Embolism Diagnosis III) Investigators. Gadolinium-enhanced magnetic resonance angiography for pulmonary embolism: a multicenter prospective study (PIOPED III). *Ann Intern Med* 2010; **152**: 434-443 [PMID: 20368649 DOI: 10.7326/0003-4819-152-7-201004060-00008]

42 **Kang KW**, Chang HJ, Kim YJ, Choi BW, Lee HS, Yang WI, Shim CY, Ha J, Chung N. Cardiac magnetic resonance imaging-derived pulmonary artery distensibility index correlates with pulmonary artery stiffness and predicts functional capacity in patients with pulmonary arterial hypertension. *Circ J* 2011; **75**: 2244-2251 [PMID: 21757816 DOI: 10.1253/circj.cj-10-1310]

43 **Ohno Y**, Koyama H, Yoshikawa T, Nishio M, Matsumoto S, Matsumoto K, Aoyama N, Nogami M, Murase K, Sugimura K. Contrast-enhanced multidetector-row computed tomography vs. Time-resolved magnetic resonance angiography vs. contrast-enhanced perfusion MRI: assessment of treatment response by patients with inoperable chronic thromboembolic pulmonary hypertension. *J Magn Reson Imaging* 2012; **36**: 612-623 [PMID: 22566188 DOI: 10.1002/jmri.23680]

44 **Ley S**, Fink C, Risse F, Ehlken N, Fischer C, Ley-Zaporozhan J, Kauczor HU, Klose H, Gruenig E. Magnetic resonance imaging to assess the effect of exercise training on pulmonary perfusion and blood flow in patients with pulmonary hypertension. *Eur Radiol* 2013; **23**: 324-331 [PMID: 22886553 DOI: 10.1007/s00330-012-2606-z]

45 **Rajaram S**, Swift AJ, Telfer A, Hurdman J, Marshall H, Lorenz E, Capener D, Davies C, Hill C, Elliot C, Condliffe R, Wild JM, Kiely DG. 3D contrast-enhanced lung perfusion MRI is an effective screening tool for chronic thromboembolic pulmonary hypertension: results from the ASPIRE Registry. *Thorax* 2013; **68**: 677-678 [PMID: 23349220 DOI: 10.1136/thoraxjnl-2012-203020]

46 **Revel MP**, Sanchez O, Lefort C, Meyer G, Couchon S, Hernigou A, Niarra R, Chatellier G, Frija G. Diagnostic accuracy of unenhanced, contrast-enhanced perfusion and angiographic MRI sequences for pulmonary embolism diagnosis: results of independent sequence readings. *Eur Radiol* 2013; **23**: 2374-2382 [PMID: 23652845 DOI: 10.1007/s00330-013-2852-8]

47 **Sugimoto M**, Kajino H, Kajihama A, Nakau K, Murakami N, Azuma H. Assessment of pulmonary arterial pressure by velocity-encoded cine magnetic resonance imaging in children with congenital heart disease. *Circ J* 2013; **77**: 3015-3022 [PMID: 24088305 DOI: 10.1253/circj.cj-13-0626]

48 **Schönfeld C**, Cebotari S, Voskrebenzev A, Gutberlet M, Hinrichs J, Renne J, Hoeper MM, Olsson KM, Welte T, Wacker F, Vogel-Claussen J. Performance of perfusion-weighted Fourier decomposition MRI for detection of chronic pulmonary emboli. *J Magn Reson Imaging* 2015; **42**: 72-79 [PMID: 25227559 DOI: 10.1002/jmri.24764]

49 **Ingrisch M**, Maxien D, Meinel FG, Reiser MF, Nikolaou K, Dietrich O. Detection of pulmonary embolism with free-breathing dynamic contrast-enhanced MRI. *J Magn Reson Imaging* 2016; **43**: 887-893 [PMID: 26391931 DOI: 10.1002/jmri.25050]

50 **Johns CS**, Swift AJ, Rajaram S, Hughes PJC, Capener DJ, Kiely DG, Wild JM. Lung perfusion: MRI vs. SPECT for screening in suspected chronic thromboembolic pulmonary hypertension. *J Magn Reson Imaging* 2017; **46**: 1693-1697 [PMID: 28376242 DOI: 10.1002/jmri.25714]

51 **Voskrebenzev A**, Gutberlet M, Klimeš F, Kaireit TF, Schönfeld C, Rotärmel A, Wacker F, Vogel-Claussen J. Feasibility of quantitative regional ventilation and perfusion mapping with phase-resolved functional lung (PREFUL) MRI in healthy volunteers and COPD, CTEPH, and CF patients. *Magn Reson Med* 2018; **79**: 2306-2314 [PMID: 28856715 DOI: 10.1002/mrm.26893]

52 **Agoston-Coldea L**, Lupu S, Mocan T. Pulmonary Artery Stiffness by Cardiac Magnetic Resonance Imaging Predicts Major Adverse Cardiovascular Events in patients with Chronic Obstructive Pulmonary Disease. *Sci Rep* 2018; **8**: 14447 [PMID: 30262820 DOI: 10.1038/s41598-018-32784-6]

53 **Schoenfeld C**, Hinrichs JB, Olsson KM, Kuettner MA, Renne J, Kaireit T, Czerner C, Wacker F, Hoeper MM, Meyer BC, Vogel-Claussen J. Cardio-pulmonary MRI for detection of treatment response after a single BPA treatment session in CTEPH patients. *Eur Radiol* 2019; **29**: 1693-1702 [PMID: 30311032 DOI: 10.1007/s00330-018-5696-4]

54 **Moher Alsady T**, Kaireit TF, Behrendt L, Winther HB, Olsson KM, Wacker F, Hoeper MM, Cebotari S, Vogel-Claussen J. Comparison of dual-energy computer tomography and dynamic contrast-enhanced MRI for evaluating lung perfusion defects in chronic thromboembolic pulmonary hypertension. *PLoS One* 2021; **16**: e0251740 [PMID: 34138864 DOI: 10.1371/journal.pone.0251740]

55 **Torres LA**, Lee KE, Barton GP, Hahn AD, Sandbo N, Schiebler ML, Fain SB. Dynamic contrast enhanced MRI for the evaluation of lung perfusion in idiopathic pulmonary fibrosis. *Eur Respir J* 2022; **60** [PMID: 35273033 DOI: 10.1183/13993003.02058-2021]

56 **Yousaf T**, Dervenoulas G, Politis M. Advances in MRI Methodology. *Int Rev Neurobiol* 2018; **141**: 31-76 [PMID: 30314602 DOI: 10.1016/bs.irn.2018.08.008]

57 **Hatabu H**, Ohno Y, Gefter WB, Parraga G, Madore B, Lee KS, Altes TA, Lynch DA, Mayo JR, Seo JB, Wild JM, van Beek EJR, Schiebler

ML, Kauczor HU; Fleischner Society. Expanding Applications of Pulmonary MRI in the Clinical Evaluation of Lung Disorders: Fleischner Society Position Paper. *Radiology* 2020; **297**: 286-301 [PMID: 32870136 DOI: 10.1148/radiol.2020201138]

58 **Alsop DC**, Hatabu H, Bonnet M, Listerud J, Gefter W. Multi-slice, breathhold imaging of the lung with submillisecond echo times. *Magn Reson Med* 1995; **33**: 678-682 [PMID: 7596272 DOI: 10.1002/mrm.1910330513]

59 **Mayo JR**, MacKay A, Müller NL. MR imaging of the lungs: value of short TE spin-echo pulse sequences. *AJR Am J Roentgenol* 1992; **159**: 951-956 [PMID: 1414805 DOI: 10.2214/ajr.159.5.1414805]

60 **Gordon Y**, Partovi S, Müller-Eschner M, Amarteifio E, Bäuerle T, Weber MA, Kauczor HU, Rengier F. Dynamic contrast-enhanced magnetic resonance imaging: fundamentals and application to the evaluation of the peripheral perfusion. *Cardiovasc Diagn Ther* 2014; **4**: 147-164 [PMID: 24834412 DOI: 10.3978/j.issn.2223-3652.2014.03.01]

61 **Patel SH**, Batchala PP, Schallert K, Patrie JT, Abbas SO, Ornan DA, Mukherjee S, Huerta T, Mugler JP 3rd. 3D fast low-angle shot (FLASH) technique for 3T contrast-enhanced brain MRI in the inpatient and emergency setting: comparison with 3D magnetization-prepared rapid gradient echo (MPRAGE) technique. *Neuroradiology* 2021; **63**: 897-904 [PMID: 33118042 DOI: 10.1007/s00234-020-02590-x]

62 **Cuenod CA**, Balvay D. Perfusion and vascular permeability: basic concepts and measurement in DCE-CT and DCE-MRI. *Diagn Interv Imaging* 2013; **94**: 1187-1204 [PMID: 24211260 DOI: 10.1016/j.diii.2013.10.010]

63 **Rajaram S**, Swift AJ, Capener D, Telfer A, Davies C, Hill C, Condliffe R, Elliot C, Hurdman J, Kiely DG, Wild JM. Diagnostic accuracy of contrast-enhanced MR angiography and unenhanced proton MR imaging compared with CT pulmonary angiography in chronic thromboembolic pulmonary hypertension. *Eur Radiol* 2012; **22**: 310-317 [PMID: 21887483 DOI: 10.1007/s00330-011-2252-x]

64 **Deshmane A**, Gulani V, Griswold MA, Seiberlich N. Parallel MR imaging. *J Magn Reson Imaging* 2012; **36**: 55-72 [PMID: 22696125 DOI: 10.1002/jmri.23639]

65 **Nazir MS**, Neji R, Speier P, Reid F, Stäb D, Schmidt M, Forman C, Razavi R, Plein S, Ismail TF, Chiribiri A, Roujol S. Simultaneous multi slice (SMS) balanced steady state free precession first-pass myocardial perfusion cardiovascular magnetic resonance with iterative reconstruction at 1.5 T. *J Cardiovasc Magn Reson* 2018; **20**: 84 [PMID: 30526627 DOI: 10.1186/s12968-018-0502-7]

66 **Kellman P**, Hansen MS, Nielles-Vallespin S, Nickander J, Themudo R, Ugander M, Xue H. Myocardial perfusion cardiovascular magnetic resonance: optimized dual sequence and reconstruction for quantification. *J Cardiovasc Magn Reson* 2017; **19**: 43 [PMID: 28385161 DOI: 10.1186/s12968-017-0355-5]

67 **Ingrisch M**, Maxien D, Schwab F, Reiser MF, Nikolaou K, Dietrich O. Assessment of pulmonary perfusion with breath-hold and free-breathing dynamic contrast-enhanced magnetic resonance imaging: quantification and reproducibility. *Invest Radiol* 2014; **49**: 382-389 [PMID: 24473368 DOI: 10.1097/RLI.0000000000000020]

68 **Maxien D**, Ingrisch M, Meinel FG, Reiser M, Dietrich O, Nikolaou K. Quantification of pulmonary perfusion with free-breathing dynamic contrast-enhanced MRI--a pilot study in healthy volunteers. *Rofo* 2013; **185**: 1175-1181 [PMID: 23884909 DOI: 10.1055/s-0033-1350128]

69 **Borhani AA**, Hosseinzadeh K. Quantitative Versus Qualitative Methods in Evaluation of T2 Signal Intensity to Improve Accuracy in Diagnosis of Pheochromocytoma. *AJR Am J Roentgenol* 2015; **205**: 302-310 [PMID: 26204279 DOI: 10.2214/AJR.14.13273]

70 **Villa ADM**, Corsinovi L, Ntalas I, Milidonis X, Scannell C, Di Giovine G, Child N, Ferreira C, Nazir MS, Karady J, Eshja E, De Francesco V, Bettencourt N, Schuster A, Ismail TF, Razavi R, Chiribiri A. Importance of operator training and rest perfusion on the diagnostic accuracy of stress perfusion cardiovascular magnetic resonance. *J Cardiovasc Magn Reson* 2018; **20**: 74 [PMID: 30454074 DOI: 10.1186/s12968-018-0493-4]

71 **Jerosch-Herold M**. Quantification of myocardial perfusion by cardiovascular magnetic resonance. *J Cardiovasc Magn Reson* 2010; **12**: 57 [PMID: 20932314 DOI: 10.1186/1532-429X-12-57]

72 **Jerosch-Herold M**, Wilke N, Stillman AE. Magnetic resonance quantification of the myocardial perfusion reserve with a Fermi function model for constrained deconvolution. *Med Phys* 1998; **25**: 73-84 [PMID: 9472829 DOI: 10.1118/1.598163]

73 **Zierler K**. Indicator dilution methods for measuring blood flow, volume, and other properties of biological systems: a brief history and memoir. *Ann Biomed Eng* 2000; **28**: 836-848 [PMID: 11144667 DOI: 10.1114/1.1308496]

74 **Calamante F**. Arterial input function in perfusion MRI: a comprehensive review. *Prog Nucl Magn Reson Spectrosc* 2013; **74**: 1-32 [PMID: 24083460 DOI: 10.1016/j.pnmrs.2013.04.002]

75 **Ishida M**, Schuster A, Morton G, Chiribiri A, Hussain S, Paul M, Merkle N, Steen H, Lossnitzer D, Schnackenburg B, Alfakih K, Plein S, Nagel E. Development of a universal dual-bolus injection scheme for the quantitative assessment of myocardial perfusion cardiovascular magnetic resonance. *J Cardiovasc Magn Reson* 2011; **13**: 28 [PMID: 21609423 DOI: 10.1186/1532-429X-13-28]

76 **Risse F**, Semmler W, Kauczor HU, Fink C. Dual-bolus approach to quantitative measurement of pulmonary perfusion by contrast-enhanced MRI. *J Magn Reson Imaging* 2006; **24**: 1284-1290 [PMID: 17051533 DOI: 10.1002/jmri.20747]

77 **Broadbent DA**, Biglands JD, Ripley DP, Higgins DM, Greenwood JP, Plein S, Buckley DL. Sensitivity of quantitative myocardial dynamic contrast-enhanced MRI to saturation pulse efficiency, noise and t1 measurement error: Comparison of nonlinearity correction methods. *Magn Reson Med* 2016; **75**: 1290-1300 [PMID: 25946025 DOI: 10.1002/mrm.25726]

78 **Gatehouse PD**, Elkington AG, Ablitt NA, Yang GZ, Pennell DJ, Firmin DN. Accurate assessment of the arterial input function during high-dose myocardial perfusion cardiovascular magnetic resonance. *J Magn Reson Imaging* 2004; **20**: 39-45 [PMID: 15221807 DOI: 10.1002/jmri.20054]

79 **Jahng GH**, Li KL, Ostergaard L, Calamante F. Perfusion magnetic resonance imaging: a comprehensive update on principles and techniques. *Korean J Radiol* 2014; **15**: 554-577 [PMID: 25246817 DOI: 10.3348/kjr.2014.15.5.554]

80 **Schoenfeld C**, Cebotari S, Hinrichs J, Renne J, Kaireit T, Olsson KM, Voskrebenzev A, Gutberlet M, Hoeper MM, Welte T, Haverich A, Wacker F, Vogel-Claussen J. MR Imaging-derived Regional Pulmonary Parenchymal Perfusion and Cardiac Function for Monitoring Patients with Chronic Thromboembolic Pulmonary Hypertension before and after Pulmonary Endarterectomy. *Radiology* 2016; **279**: 925-934 [PMID: 26727392 DOI: 10.1148/radiol.2015150765]

81 **Altes TA**, Rehm PK, Harrell F, Salerno M, Daniel TM, De Lange EE. Ventilation imaging of the lung: comparison of hyperpolarized helium-3 MR imaging with Xe-133 scintigraphy. *Acad Radiol* 2004; **11**: 729-734 [PMID: 15217589 DOI: 10.1016/j.acra.2004.04.001]

82 **Marshall H**, Kiely DG, Parra-Robles J, Capener D, Deppe MH, van Beek EJ, Swift AJ, Rajaram S, Hurdman J, Condliffe R, Elliot CA, Wild JM. Magnetic resonance imaging of ventilation and perfusion changes in response to pulmonary endarterectomy in chronic thromboembolic pulmonary hypertension. *Am J Respir Crit Care Med* 2014; **190**: e18-e19 [PMID: 25171318 DOI: 10.1164/rccm.201310-1842IM]

83 **Saunders LC**, Hughes PJC, Alabed S, Capener DJ, Marshall H, Vogel-Claussen J, van Beek EJR, Kiely DG, Swift AJ, Wild JM. Integrated Cardiopulmonary MRI Assessment of Pulmonary Hypertension. *J Magn Reson Imaging* 2022; **55**: 633-652 [PMID: 34350655 DOI: 10.1002/jmri.27849]

84 **Wang Z**, He M, Bier E, Rankine L, Schrank G, Rajagopal S, Huang YC, Kelsey C, Womack S, Mammarappallil J, Driehuys B. Hyperpolarized (129) Xe gas transfer MRI: the transition from 1.5T to 3T. *Magn Reson Med* 2018; **80**: 2374-2383 [PMID: 30024058 DOI: 10.1002/mrm.27377]

85 **Dahhan T**, Kaushik SS, He M, Mammarappallil JG, Tapson VF, McAdams HP, Sporn TA, Driehuys B, Rajagopal S. Abnormalities in hyperpolarized (129)Xe magnetic resonance imaging and spectroscopy in two patients with pulmonary vascular disease. *Pulm Circ* 2016; **6**: 126-131 [PMID: 27162620 DOI: 10.1086/685110]

86 **Wang Z**, Bier EA, Swaminathan A, Parikh K, Nouls J, He M, Mammarappallil JG, Luo S, Driehuys B, Rajagopal S. Diverse cardiopulmonary diseases are associated with distinct xenon magnetic resonance imaging signatures. *Eur Respir J* 2019; **54** [PMID: 31619473 DOI: 10.1183/13993003.00831-2019]

87 **U-King-Im JM**, Freeman SJ, Boylan T, Cheow HK. Quality of CT pulmonary angiography for suspected pulmonary embolus in pregnancy. *Eur Radiol* 2008; **18**: 2709-2715 [PMID: 18651151 DOI: 10.1007/s00330-008-1100-0]

88 **Mehra P**, Mehta V, Sukhija R, Sinha AK, Gupta M, Girish MP, Aronow WS. Pulmonary hypertension in left heart disease. *Arch Med Sci* 2019; **15**: 262-273 [PMID: 30697278 DOI: 10.5114/aoms.2017.68938]

89 **Rosenkranz S**, Howard LS, Gomberg-Maitland M, Hoeper MM. Systemic Consequences of Pulmonary Hypertension and Right-Sided Heart Failure. *Circulation* 2020; **141**: 678-693 [PMID: 32091921 DOI: 10.1161/CIRCULATIONAHA.116.022362]

90 **Calderaro D**, Alves Junior JL, Fernandes CJCDS, Souza R. Pulmonary Hypertension in General Cardiology Practice. *Arq Bras Cardiol* 2019; **113**: 419-428 [PMID: 31621783 DOI: 10.5935/abc.20190188]

91 **Swift AJ**, Capener D, Johns C, Hamilton N, Rothman A, Elliot C, Condliffe R, Charalampopoulos A, Rajaram S, Lawrie A, Campbell MJ, Wild JM, Kiely DG. Magnetic Resonance Imaging in the Prognostic Evaluation of Patients with Pulmonary Arterial Hypertension. *Am J Respir Crit Care Med* 2017; **196**: 228-239 [PMID: 28328237 DOI: 10.1164/rccm.201611-2365OC]

92 **Yun CH**, Tsai JP, Tsai CT, Mok GS, Sun JY, Hung CL, Wu TH, Huang WT, Yang FS, Lee JJ, Cury RC, Fares A, Nshisso LD, Bezerra HG. Qualitative and semi-quantitative evaluation of myocardium perfusion with 3 T stress cardiac MRI. *BMC Cardiovasc Disord* 2015; **15**: 164 [PMID: 26642757 DOI: 10.1186/s12872-015-0159-1]

93 **Wei X**, Warfield SK, Zou KH, Wu Y, Li X, Guimond A, Mugler JP 3rd, Benson RR, Wolfson L, Weiner HL, Guttmann CR. Quantitative analysis of MRI signal abnormalities of brain white matter with high reproducibility and accuracy. *J Magn Reson Imaging* 2002; **15**: 203-209 [PMID: 11836778 DOI: 10.1002/jmri.10053]

94 **Hasebroock KM**, Serkova NJ. Toxicity of MRI and CT contrast agents. *Expert Opin Drug Metab Toxicol* 2009; **5**: 403-416 [PMID: 19368492 DOI: 10.1517/17425250902873796]

95 **Webb JA**, Thomsen HS, Morcos SK; Members of Contrast Media Safety Committee of European Society of Urogenital Radiology (ESUR). The use of iodinated and gadolinium contrast media during pregnancy and lactation. *Eur Radiol* 2005; **15**: 1234-1240 [PMID: 15609057 DOI: 10.1007/s00330-004-2583-y]

96 **Salvi R**, Sheppard A. Is Noise in the MR Imager a Significant Risk Factor for Hearing Loss? *Radiology* 2018; **286**: 609-610 [PMID: 29356640 DOI: 10.1148/radiol.2017172221]

97 **Serai SD**, Hu HH, Ahmad R, White S, Pednekar A, Anupindi SA, Lee EY. Newly Developed Methods for Reducing Motion Artifacts in Pediatric Abdominal MRI: Tips and Pearls. *AJR Am J Roentgenol* 2020; **214**: 1042-1053 [PMID: 32023117 DOI: 10.2214/AJR.19.21987]

98 **Scannell CM**, Correia T, Villa ADM, Schneider T, Lee J, Breeuwer M, Chiribiri A, Henningsson M. Feasibility of free-breathing quantitative myocardial perfusion using multi-echo Dixon magnetic resonance imaging. *Sci Rep* 2020; **10**: 12684 [PMID: 32728198 DOI: 10.1038/s41598-020-69747-9]

99 **McElroy S**, Ferrazzi G, Nazir MS, Evans C, Ferreira J, Bosio F, Mughal N, Kunze KP, Neji R, Speier P, Stäb D, Ismail TF, Masci PG, Villa ADM, Razavi R, Chiribiri A, Roujol S. Simultaneous multislice steady-state free precession myocardial perfusion with full left ventricular coverage and high resolution at 1.5 T. *Magn Reson Med* 2022; **88**: 663-675 [PMID: 35344593 DOI: 10.1002/mrm.29229]

100 **Ley S**, Ley-Zaporozhan J. Pulmonary perfusion imaging using MRI: clinical application. *Insights Imaging* 2012; **3**: 61-71 [PMID: 22695999 DOI: 10.1007/s13244-011-0140-1]

101 **Lasch F**, Karch A, Koch A, Derlin T, Voskrebenzev A, Alsady TM, Hoeper MM, Gall H, Roller F, Harth S, Steiner D, Krombach G, Ghofrani HA, Rengier F, Heußel CP, Grünig E, Beitzke D, Hacker M, Lang IM, Behr J, Bartenstein P, Dinkel J, Schmidt KH, Kreitner KF, Frauenfelder T, Ulrich S, Hamer OW, Pfeifer M, Johns CS, Kiely DG, Swift AJ, Wild J, Vogel-Claussen J. Comparison of MRI and VQ-SPECT as a Screening Test for Patients With Suspected CTEPH: CHANGE-MRI Study Design and Rationale. *Front Cardiovasc Med* 2020; **7**: 51 [PMID: 32328500 DOI: 10.3389/fcvm.2020.00051]

102 **Lechartier B**, Chaouat A, Aubert JD, Schwitter J; Swiss Society for Pulmonary Hypertension (SSPH). Magnetic resonance imaging in pulmonary hypertension: an overview of current applications and future perspectives. *Swiss Med Wkly* 2022; **152**: w30055 [PMID: 35262319 DOI: 10.4414/smw.2022.w30055]

103 **Ota H**, Sugimura K, Miura M, Shimokawa H. Four-dimensional flow magnetic resonance imaging visualizes drastic change in vortex flow in the main pulmonary artery after percutaneous transluminal pulmonary angioplasty in a patient with chronic thromboembolic pulmonary hypertension. *Eur Heart J* 2015; **36**: 1630 [PMID: 25736251 DOI: 10.1093/eurheartj/ehv054]

104 **Jacobs M**, Benovoy M, Chang LC, Corcoran D, Berry C, Arai AE, Hsu LY. Automated Segmental Analysis of Fully Quantitative Myocardial Blood Flow Maps by First-Pass Perfusion Cardiovascular Magnetic Resonance. *IEEE Access* 2021; **9**: 52796-52811 [PMID: 33996344 DOI: 10.1109/access.2021.3070320]

105 **Scannell CM**, Veta M, Villa ADM, Sammut EC, Lee J, Breeuwer M, Chiribiri A. Deep-Learning-Based Preprocessing for Quantitative Myocardial Perfusion MRI. *J Magn Reson Imaging* 2020; **51**: 1689-1696 [PMID: 31710769 DOI: 10.1002/jmri.26983]

106 **Xue H**, Davies RH, Brown LAE, Knott KD, Kotecha T, Fontana M, Plein S, Moon JC, Kellman P. Automated Inline Analysis of Myocardial Perfusion MRI with Deep Learning. *Radiol Artif Intell* 2020; **2**: e200009 [PMID: 33330849 DOI: 10.1148/ryai.2020200009]

107 **Weng AM**, Heidenreich JF, Metz C, Veldhoen S, Bley TA, Wech T. Deep learning-based segmentation of the lung in MR-images acquired by a stack-of-spirals trajectory at ultra-short echo-times. *BMC Med Imaging* 2021; **21**: 79 [PMID: 33964892 DOI: 10.1186/s12880-021-00608-1]

108 **Mairhörmann B**, Castelblanco A, Häfner F, Pfahler V, Haist L, Waibel D, Flemmer A, Ehrhardt H, Stoecklein S, Dietrich O, Foerster K, Hilgendorff A, Schubert B. Deep Learning-Based Magnetic Resonance Imaging Lung Segmentation and Volumetric Marker Extraction in Preterm Infants. 2021 Preprint. Available from: medRxiv 2021.08.06.21261648 [DOI: 10.1101/2021.08.06.21261648]

World Journal of Radiology

Submit a Manuscript: https://www.f6publishing.com

World J Radiol 2023 September 28; 15(9): 274-280

DOI: 10.4329/wjr.v15.i9.274

ISSN 1949-8470 (online)

CASE REPORT

Distinctive magnetic resonance imaging features in primary central nervous system lymphoma: A case report

Li-Hong Liu, Han-Wen Zhang, Hong-Bo Zhang, Xiao-Lei Liu, Hua-Zhen Deng, Fan Lin, Biao Huang

Specialty type: Radiology, nuclear medicine and medical imaging

Provenance and peer review: Unsolicited article; Externally peer reviewed.

Peer-review model: Single blind

Peer-review report's scientific quality classification

Grade A (Excellent): 0
Grade B (Very good): B
Grade C (Good): 0
Grade D (Fair): D
Grade E (Poor): 0

P-Reviewer: Mahmoud MZ, Saudi Arabia

Received: June 30, 2023
Peer-review started: June 30, 2023
First decision: August 24, 2023
Revised: September 4, 2023
Accepted: September 22, 2023
Article in press: September 22, 2023
Published online: September 28, 2023

Li-Hong Liu, Han-Wen Zhang, Xiao-Lei Liu, Hua-Zhen Deng, Fan Lin, Department of Radiology, The First Affiliated Hospital of Shenzhen University, Health Science Center, Shenzhen Second People's Hospital, Shenzhen 518036, Guangdong Province, China

Han-Wen Zhang, Hong-Bo Zhang, Biao Huang, The Second School of Clinical Medicine, Southern Medical University, Guangzhou 510282, Guangdong Province, China

Hong-Bo Zhang, Department of Radiology, Sun Yat-Sen University, Shenzhen 518000, Guangdong Province, China

Biao Huang, Department of Radiology, Guangdong Provincial People's Hospital, Guangdong Academy of Medical Sciences, Guangzhou 510000, Guangdong Province, China

Corresponding author: Han-Wen Zhang, MD, Doctor, Department of Radiology, The First Affiliated Hospital of Shenzhen University, Health Science Center, Shenzhen Second People's Hospital, No. 3002 Sungangxi Road, Shenzhen 518036, Guangdong Province, China.
zhwstarcraft@outlook.com

Abstract

BACKGROUND

Primary central nervous system lymphoma (PCNSL) is a rare malignant tumor originating from the lymphatic hematopoietic system. It exhibits unique imaging manifestations due to its biological characteristics.

CASE SUMMARY

Magnetic resonance imaging (MRI) with diffusion-weighted imaging (DWI), perfusion-weighted imaging (PWI), and magnetic resonance spectroscopy was performed. The imaging findings showed multiple space-occupying lesions with low signal on T1-weighted imaging, uniform high signal on T2-weighted imaging, and obvious enhancement on contrast-enhanced scans. DWI revealed diffusion restriction, PWI demonstrated hypoperfusion, and spectroscopy showed elevated choline peak and decreased N-acetylaspartic acid. The patient's condition significantly improved after hormone shock therapy.

CONCLUSION

This case highlights the distinctive imaging features of PCNSL and their importance in accurate diagnosis and management.

Key Words: Primary central nervous system lymphoma; Primary central nervous system

lymphoma; Diffusion-weighted imaging; Perfusion-weighted imaging; Magnetic resonance imaging; Case report

Core Tip: Primary central nervous system lymphoma (PCNSL) is a rare tumor of the central nervous system with distinctive imaging features. This case report highlights the imaging manifestations of multiple PCNSL lesions using diffusion-weighted imaging, perfusion-weighted imaging, and magnetic resonance imaging. Accurate diagnosis is crucial for appropriate management. Further research and larger studies are needed to enhance the understanding and diagnostic accuracy of PCNSL.

Citation: Liu LH, Zhang HW, Zhang HB, Liu XL, Deng HZ, Lin F, Huang B. Distinctive magnetic resonance imaging features in primary central nervous system lymphoma: A case report. *World J Radiol* 2023; 15(9): 274-280
URL: https://www.wjgnet.com/1949-8470/full/v15/i9/274.htm
DOI: https://dx.doi.org/10.4329/wjr.v15.i9.274

INTRODUCTION

Primary central nervous system lymphoma (PCNSL) is an exceptionally rare and aggressive malignancy originating within the central nervous system. Despite its infrequency, PCNSL presents unique diagnostic and therapeutic challenges, rendering it a subject of profound clinical importance[1]. In recent years, advanced imaging techniques, including diffusion-weighted imaging (DWI), perfusion-weighted imaging (PWI), and magnetic resonance (MR) spectroscopy, have greatly enhanced our ability to comprehend the disease and its distinctive manifestations[2].

While previous studies have provided valuable insights into the broader understanding of PCNSL, there is a critical gap in characterizing the imaging features on an individual case level[3]. This study endeavors to bridge this gap by conducting an in-depth examination of DWI, PWI, and MR spectroscopy findings in a single PCNSL case. By scrutinizing these imaging modalities within the unique context of this individual case, we aim to contribute to the comprehensive understanding of PCNSL's imaging features and their potential clinical implications[4].

The primary research problem addressed in this study is to delineate the specific magnetic resonance imaging (MRI) imaging manifestations of PCNSL within the scope of a single case analysis and to comprehend their diagnostic and clinical significance. To accomplish this, we have conducted a detailed analysis of DWI, PWI, and MR spectroscopy findings in the context of this singular PCNSL case.

CASE PRESENTATION

Chief complaints

A 79-year-old female patient with a previously unremarkable medical history presented with a sudden onset of unexplained dizziness accompanied by projectile vomiting, characterized by the ejection of gastric contents. She also reported a sense of heaviness and weakness in her limbs.

History of present illness

Initial evaluation at another medical facility revealed the presence of multiple intracranial space-occupying lesions. These lesions were detected through a computed tomography scan, which indicated the involvement of the cerebellar hemisphere, corpus callosum's splenium, and the left parietal lobe.

History of past illness

No special notes.

Personal and family history

No special notes.

Physical examination

Physical examination revealed no abnormalities.

Laboratory examinations

The platelet specific volume was slightly elevated. The monocyte count was mildly elevated. The bacterial content in the urine test increased [4225.40, reference value: 0-4000 (/μL)].

Imaging examinations

Upon admission, the patient underwent a comprehensive evaluation, including MRI with DWI, PWI, and MR spectroscopy (MRS). The MRI results confirmed the presence of multiple space-occupying lesions, characterized by low signal intensity on T1-weighted imaging, uniform high signal intensity on T2-weighted imaging, and prominent enhancement on contrast-enhanced scans (Figure 1). DWI further revealed diffusion restriction, while PWI demonstrated hypoperfusion in all the identified lesions. Additionally, spectroscopy (MRS) depicted an elevated choline peak and decreased N-acetylaspartic acid. Notably, MRS also revealed the presence of a Lip peak within the lesion (Figure 2). These combined imaging features strongly suggested the possibility of PCNSL.

FINAL DIAGNOSIS

Pathological examination of the intracranial lesion confirmed the presence of an aggressive B-cell lymphoma. Immunohistochemical analysis demonstrated the following profile: CD21 (-), CD10 (-), CD20 (+), CD3 (background T-cells +), CD30 (-), PAX-5 (+), Bcl-6 (+), MUM-1 (+), Ki-67 (approximately 80%), CD5 (-), CD23 (-), Bcl-2 (-), CyclinD1 (-), CD79A (+), C-MYC (approximately 30%+), P53 (10%+ with varying intensity), GFAP (glial cells +). Importantly, Epstein-Barr virus-encoded small RNA (EBER) was not detected. These findings confirmed the diagnosis of diffuse large B-cell lymphoma of the non-germinal center B-cell (non-GCB) subtype, supporting the diagnosis of PCNSL.

TREATMENT

Treatment and response

In response to the initial presentation and MRI findings, the patient underwent a diagnostic trial of steroid therapy. This treatment led to a significant improvement in the patient's neurological condition, although it was accompanied by the emergence of certain neuropsychiatric symptoms. Subsequent administration of medications, including lorazepam and olanzapine, resulted in a notable improvement in the patient's neuropsychiatric symptoms. Follow-up MRI examinations indicated a reduction in enhancement in the lesions located in the hippocampus and left parietal lobe, with the other lesions remaining stable or showing slight reductions (Figure 3).

OUTCOME AND FOLLOW-UP

The patient subsequently received standardized lymphoma immunotherapy and chemotherapy regimens, and her prognosis remains favorable.

DISCUSSION

There is no lymphoid tissue present within the central nervous system, making brain lymphomas relatively rare. Currently, the origin of intracerebral lymphoma can be attributed to the following factors: Firstly, reactive lymphocytes enter the brain tissue during intracerebral infection and undergo malignant transformation through various mechanisms. Secondly, activated peripheral lymphocytes transform into tumor cells and migrate to the brain through the bloodstream, resulting in tumors primarily located around the ventricles, basal ganglia, and frontoparietal lobes. Thirdly, undifferentiated pluripotent stem cells surrounding blood vessels in the brain may serve as the source of intracerebral lymphoma. Histologically, intracerebral lymphomas exhibit predominant sleeve-shaped growth, infiltrating the surrounding brain parenchyma, and demonstrating multicentric growth within the tumor[5].

PCNSL typically presents as supratentorial lesions, with predilection sites in the cerebral hemisphere, corpus callosum, basal ganglia, and thalamus[6]. The imaging findings of PCNSL are closely related to its pathological features. In this case, the lesions were confined to the brain tissue, involving both supratentorial and infratentorial areas, which is relatively rare[7].

On conventional MRI, PCNSL shows iso-hypointensity on T1-weighted imaging and iso-hypointensity on T2-weighted imaging[8]. DWI demonstrates diffusion restriction due to densely arranged tumor cells. According to Lin *et al*[9], their study suggests that combining DWI ADC value with T1WI enhanced scan can aid in the differentiation of glioblastoma from PCNSL. PWI reveals hypoperfusion, reflecting the hypo-vascular nature of PCNSL[10]. Contrast-enhanced scans show uniform enhancement when the tumor invades adjacent brain parenchyma and disrupts the blood-brain barrier (BBB). In our previous study, we compared high-grade glioma (HGG) with lymphoma using dynamic contrast-enhanced (DCE) imaging, and found that lymphoma has more obvious damage to the BBB, resulting in transfer constant(K^{trans}) values even higher than HGG[11]. The characteristic imaging features, such as the "fist sign," "sharp horn sign," and "butterfly wing sign,"(usually occurs in the corpus callosum) are associated with the tumor's angiophilic growth.

MRS plays a crucial role in the evaluation of PCNSL. Elevated choline peak, decreased N-acetylaspartic acid, and a towering lipid peak are commonly observed[12]. The towering lipid peak is highly specific for the diagnosis of PCNSL, attributed to the accelerated turnover of lymphocytes and macrophages. PCNSL should be differentiated from

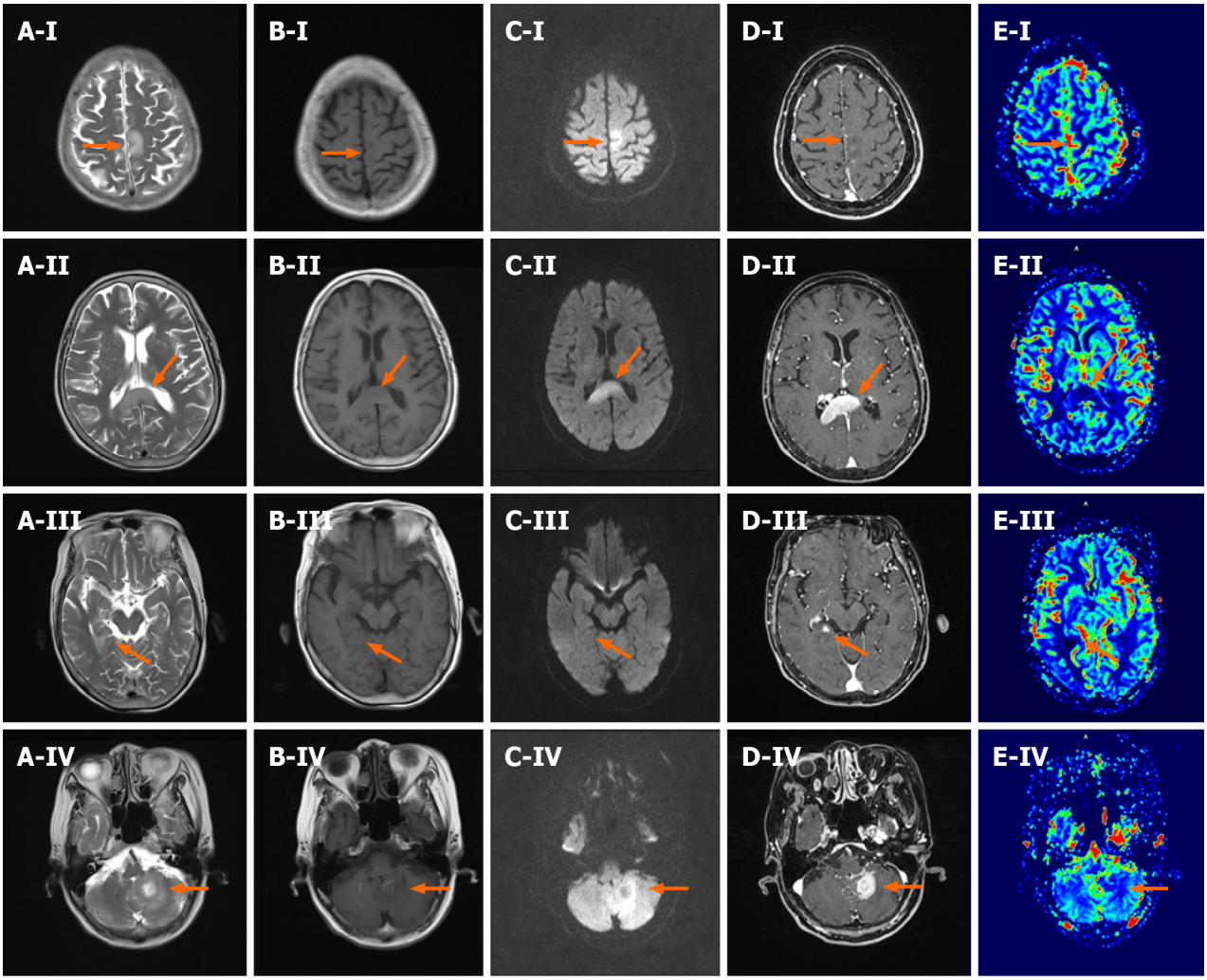

DOI: 10.4329/wjr.v15.i9.274 **Copyright** ©The Author(s) 2023.

Figure 1 Images of the patient prior to corticosteroid pulse therapy. A: T2WI; B: T1WI; C: Diffusion-weighted imaging; D: T1-weighted enhanced scan; E: Dynamic susceptibility contrast perfusion-weighted imaging cerebral blood volume; I: parietal lobe lesions; II: corpus callosum lesions; III: hippocampal lesions; IV: Left cerebellar hemisphere lesions.

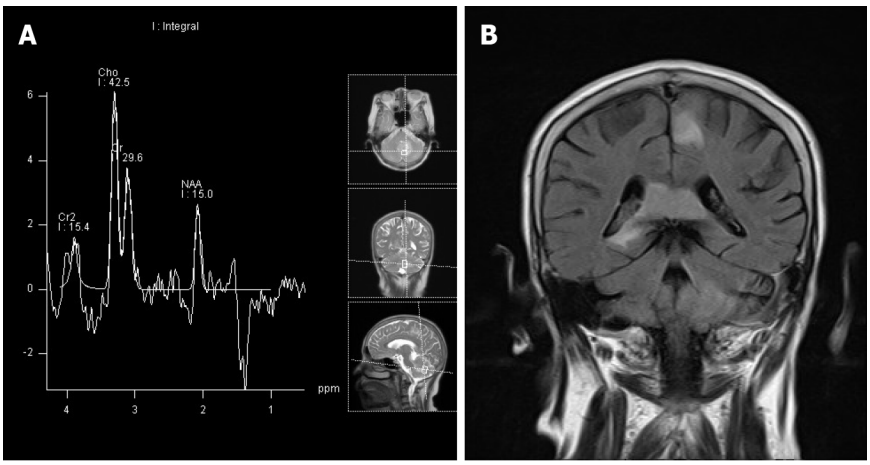

DOI: 10.4329/wjr.v15.i9.274 **Copyright** ©The Author(s) 2023.

Figure 2 Notably, magnetic resonance spectroscopy also revealed the presence of a lip peak within the lesion. A: Magnetic resonance spectroscopy; B: Butterfly sign when primary central nervous system lymphoma is located in the corpus callosum.

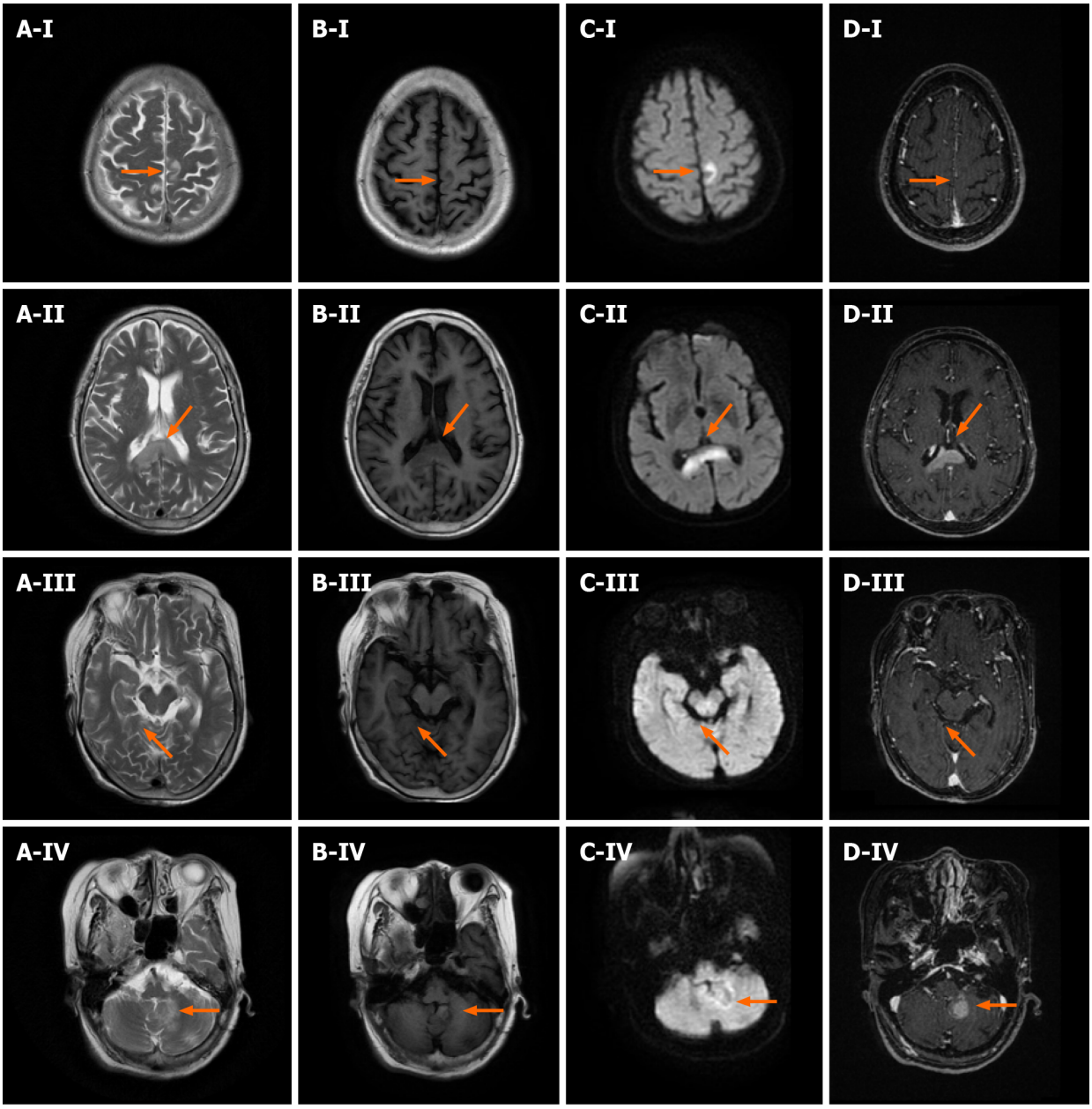

DOI: 10.4329/wjr.v15.i9.274

Figure 3 Images of the patient following corticosteroid pulse therapy. A: T2WI; B: T1WI; C: Diffusion-weighted imaging; D: T1-weighted enhanced scan; I: Parietal lobe lesions; II: Corpus callosum lesions; III: Hippocampal lesions; IV: Left cerebellar hemisphere lesions.

demyelinating diseases, as their imaging findings may resemble each other[13]. Hormone shock therapy can provide symptomatic relief in both PCNSL and demyelinating diseases, but recovery of symptoms after hormone therapy withdrawal is indicative of PCNSL.

In addition to our contributions to the understanding of PCNSL, it is essential to recognize the limitations of our study. The utilization of a single-case design inherently limits the generalizability of our findings to a broader population of PCNSL patients. Future research should strive to replicate these findings in larger cohorts to establish their broader applicability. Furthermore, our study primarily focuses on the imaging aspects of PCNSL, and future investigations could explore the correlation between imaging features and specific clinical outcomes. These considerations highlight both the strengths and the areas for improvement in our research.

CONCLUSION

This single-case analysis of PCNSL has shed light on the distinctive MRI imaging features of this rare malignancy. By employing advanced techniques such as DWI, PWI, and MR spectroscopy, we have provided a comprehensive characterization of PCNSL's imaging manifestations. However, it is important to acknowledge the limitations of this study. The use of a single-case design restricts the generalizability of our findings to a broader population. Future research should

aim to replicate these findings in larger cohorts of PCNSL patients to establish their broader applicability. Additionally, our study focused on the imaging aspects, and future investigations could explore the correlation between imaging features and specific clinical outcomes. Despite these limitations, our study contributes valuable insights into the unique imaging features of PCNSL and serves as a foundation for further research in this area.

FOOTNOTES

Author contributions: Case studies were provided by Liu LH; Zhang HW wrote the article; Deng HZ searched the literature; Zhang HB analyzed the case; Huang B and Lin F revised and reviewed the manuscript; Huang B (huangbiao@gdph.org.cn), Lin F (foxetfoxet@gmail.com), and Zhang HW contributed equally to this research.

Supported by National Natural Science Foundation of China, No. 82071871; Guangdong Basic and Applied Basic Research Foundation, No. 2021A1515220131; Guangdong Medical Science and Technology Research Fund Project, No. 2022111520491834; and Clinical Research Project of Shenzhen Second People's Hospital, China, No. 20223357022.

Informed consent statement: The patient signed an informed consent to the publication of this case.

Conflict-of-interest statement: The author(s) declared no potential conflicts of interest with respect to the research, authorship, and/or publication of this article.

CARE Checklist (2016) statement: The authors have read the CARE Checklist (2016), and the manuscript was prepared and revised according to the CARE Checklist (2016).

Country/Territory of origin: China

ORCID number: Han-Wen Zhang 0000-0001-5731-7429; Fan Lin 0000-0003-1595-2736.

S-Editor: Liu JH
L-Editor: A
P-Editor: Liu JH

REFERENCES

1 **Krebs S**, Barasch JG, Young RJ, Grommes C, Schöder H. Positron emission tomography and magnetic resonance imaging in primary central nervous system lymphoma-a narrative review. *Ann Lymphoma* 2021; **5** [PMID: 34223561 DOI: 10.21037/aol-20-52]
2 **Schaff LR**, Grommes C. Primary central nervous system lymphoma. *Blood* 2022; **140**: 971-979 [PMID: 34699590 DOI: 10.1182/blood.2020008377]
3 **Deng B**, Dai Y, Wang Q, Yang J, Chen X, Liu TT, Liu J. The clinical analysis of new-onset status epilepticus. *Epilepsia Open* 2022; **7**: 771-780 [PMID: 36214088 DOI: 10.1002/epi4.12657]
4 **Han Y**, Wang ZJ, Li WH, Yang Y, Zhang J, Yang XB, Zuo L, Xiao G, Wang SZ, Yan LF, Cui GB. Differentiation Between Primary Central Nervous System Lymphoma and Atypical Glioblastoma Based on MRI Morphological Feature and Signal Intensity Ratio: A Retrospective Multicenter Study. *Front Oncol* 2022; **12**: 811197 [PMID: 35174088 DOI: 10.3389/fonc.2022.811197]
5 **Barajas RF**, Politi LS, Anzalone N, Schöder H, Fox CP, Boxerman JL, Kaufmann TJ, Quarles CC, Ellingson BM, Auer D, Andronesi OC, Ferreri AJM, Mrugala MM, Grommes C, Neuwelt EA, Ambady P, Rubenstein JL, Illerhaus G, Nagane M, Batchelor TT, Hu LS. Consensus recommendations for MRI and PET imaging of primary central nervous system lymphoma: guideline statement from the International Primary CNS Lymphoma Collaborative Group (IPCG). *Neuro Oncol* 2021; **23**: 1056-1071 [PMID: 33560416 DOI: 10.1093/neuonc/noab020]
6 **Weller M**. The vanishing role of whole brain radiotherapy for primary central nervous system lymphoma. *Neuro Oncol* 2014; **16**: 1035-1036 [PMID: 24958097 DOI: 10.1093/neuonc/nou120]
7 **Bhattacharjee R**, Gupta M, Singh T, Sharma S, Khanna G, Parvaze SP, Patir R, Vaishya S, Ahlawat S, Singh A, Gupta RK. Role of intra-tumoral vasculature imaging features on susceptibility weighted imaging in differentiating primary central nervous system lymphoma from glioblastoma: a multiparametric comparison with pathological validation. *Neuroradiology* 2022; **64**: 1801-1818 [PMID: 35435463 DOI: 10.1007/s00234-022-02946-5]
8 **Toh CH**, Wei KC, Chang CN, Ng SH, Wong HF. Differentiation of primary central nervous system lymphomas and glioblastomas: comparisons of diagnostic performance of dynamic susceptibility contrast-enhanced perfusion MR imaging without and with contrast-leakage correction. *AJNR Am J Neuroradiol* 2013; **34**: 1145-1149 [PMID: 23348763 DOI: 10.3174/ajnr.A3383]
9 **Lin X**, Lee M, Buck O, Woo KM, Zhang Z, Hatzoglou V, Omuro A, Arevalo-Perez J, Thomas AA, Huse J, Peck K, Holodny AI, Young RJ. Diagnostic Accuracy of T1-Weighted Dynamic Contrast-Enhanced-MRI and DWI-ADC for Differentiation of Glioblastoma and Primary CNS Lymphoma. *AJNR Am J Neuroradiol* 2017; **38**: 485-491 [PMID: 27932505 DOI: 10.3174/ajnr.A5023]
10 **Kang KM**, Choi SH, Chul-Kee P, Kim TM, Park SH, Lee JH, Lee ST, Hwang I, Yoo RE, Yun TJ, Kim JH, Sohn CH. Differentiation between glioblastoma and primary CNS lymphoma: application of DCE-MRI parameters based on arterial input function obtained from DSC-MRI. *Eur*

Radiol 2021; **31**: 9098-9109 [PMID: 34003350 DOI: 10.1007/s00330-021-08044-z]

11 **Zhang HW**, Lyu GW, He WJ, Lei Y, Lin F, Feng YN, Wang MZ. Differential diagnosis of central lymphoma and high-grade glioma: dynamic contrast-enhanced histogram. *Acta Radiol* 2020; **61**: 1221-1227 [PMID: 31902220 DOI: 10.1177/0284185119896519]

12 **Du X**, He Y, Lin W. Diagnostic Accuracy of the Diffusion-Weighted Imaging Method Used in Association With the Apparent Diffusion Coefficient for Differentiating Between Primary Central Nervous System Lymphoma and High-Grade Glioma: Systematic Review and Meta-Analysis. *Front Neurol* 2022; **13**: 882334 [PMID: 35812103 DOI: 10.3389/fneur.2022.882334]

13 **Miyajima T**, Ohigashi H, Yaguchi H, Teshima T. Neurolymphomatosis in Intravascular Large B-cell Lymphoma. *Intern Med* 2023; **62**: 1381-1382 [PMID: 36198588 DOI: 10.2169/internalmedicine.0021-22]

Published by **Baishideng Publishing Group Inc**
7041 Koll Center Parkway, Suite 160, Pleasanton, CA 94566, USA
Telephone: +1-925-3991568
E-mail: bpgoffice@wjgnet.com
Help Desk: https://www.f6publishing.com/helpdesk
https://www.wjgnet.com